(2)

Research and Development Technical Report
SLCET-TR-91-3 (Rev. 1)

The Effects of Acceleration on Precision Frequency Sources

(Proposed for IEEE Standards Project P1193)

John R. Vig, U. S. Army Electronics Technology and Devices Laboratory
Claude Audoin, Université Paris-Sud
Leonard S. Cutler, Hewlett-Packard Co.
Michael M. Driscoll, Westinghouse Defense and Electronic Systems Center
Errol P. EerNisse, Quartztronics, Inc.
Raymond L. Filler, U. S. Army Electronics Technology & Devices Laboratory
R. Michael Garvey, Frequency and Time Systems, Inc.
William J. Riley, EG&G Frequency Products
Robert C. Smythe, Piezo Technology, Inc.
Rolf D. Weglein, Consultant

July 1992

U. S. ARMY LABORATORY COMMAND
Electronics Technology and Devices Laboratory
Fort Monmouth, NJ 07703-5601

NOTICES

Disclaimers

The findings in this report are not to be construed as an official Department of the Army position, unless so designated by other authorized documents.

The citation of trade names and names of manufacturers in this report is not to be construed as official Government indorsement or approval of commercial products or services referenced herein.

REPORT DOCUMENTATION PAGE

Form Approved
OMB No. 0704-0188

1. AGENCY USE ONLY (Leave blank)	2. REPORT DATE	3. REPORT TYPE AND DATES COVERED
	July 1992	Technical Report

4. TITLE AND SUBTITLE

The Effects of Acceleration on Precision Frequency Sources
(Proposed for IEEE Standards Project P1193)

5. FUNDING NUMBERS

PE: 1L1
PR: 62705
TA: AH94

6. AUTHOR(S)

John R. Vig, Claude Audoin, Leonard S. Cutler, Michael M. Driscoll, Errol P. EerNisse, Raymond L. Filler, R. Michael Garvey, William J. Riley, Robert C. Smythe, and Rolf D. Weglein.

7. PERFORMING ORGANIZATION NAME(S) AND ADDRESS(ES)

US Army Laboratory Command (LABCOM)
Electronics Technology and Devices Laboratory (ETDL)
ATTN: SLCET-EF
Fort Monmouth, NJ 07703-5601

8. PERFORMING ORGANIZATION REPORT NUMBER

SLCET-TR-91-3 (Rev. 1)

9. SPONSORING/MONITORING AGENCY NAME(S) AND ADDRESS(ES)

10. SPONSORING/MONITORING AGENCY REPORT NUMBER

11. SUPPLEMENTARY NOTES This report is a revision of a report of the same title (AD A235470), and is a preprint of a section entitled "Acceleration Effects" that has been prepared for IEEE Standards Project P1193, "Guidelines for Measurement of Environmental Sensitivities of Precision Frequency Sources." The report was prepared by Working Group 4 of the IEEE Standards Coordinating Committee 27 on Time and Frequency. SCC 27 is chaired by Helmut Hellwig, Air Force (Cont'd)

12a. DISTRIBUTION/AVAILABILITY STATEMENT

Approved for public release. Distribution is unlimited.

12b. DISTRIBUTION CODE

13. ABSTRACT *(Maximum 200 words)*

The effects of acceleration on quartz and atomic frequency sources are reviewed. Guidelines are provided for the specification and testing of oscillator acceleration sensitivities. The discussion includes: steady-state acceleration effects, gravity change effects, shock effects, and vibration effects. The vibration effects section includes: sinusoidal vibration, random vibration, acoustic noise, the effects on short term stability, and spectral responses at other than the vibration frequency.

14. SUBJECT TERMS Crystal oscillator, quartz oscillator, atomic frequency standard, atomic clock, acceleration, vibration, shock, quartz, quartz crystal oscillator, quartz resonator, rubidium frequency standard, cesium beam frequency standard, crystal filter, time, clock, frequency control, frequency standard.

15. NUMBER OF PAGES 63

16. PRICE CODE

17. SECURITY CLASSIFICATION OF REPORT	18. SECURITY CLASSIFICATION OF THIS PAGE	19. SECURITY CLASSIFICATION OF ABSTRACT	20. LIMITATION OF ABSTRACT
Unclassified	Unclassified	Unclassified	UL

11. SUPPLEMENTARY NOTES (Continued).

Office of Scientific Research. The Working Group is chaired by John R. Vig; the members of Working Group are the authors of this report: John R. Vig, U.S. Army LABCOM, ATTN: SLCET-EF, Ft. Monmouth, NJ 07703-5601; Claude Audoin, Laboratoire de L'Horloge Atomique, Batiment 221, Universite de Paris-Sud, 91405 Orsay, France; Leonard S. Cutler, Hewlett-Packard Company, 3500 Deer Creek Road, Palo Alto, CA 94304; Michael M. Driscoll, Westinghouse Defense & Electronic Systems Center, P.O. Box 746, MS 75, Baltimore, MD 21203; Errol P. EerNisse, Quartztronics, Inc., 1020 W. Atherton Dr., Bldg. C, Salt Lake City, UT 84123; Raymond L. Filler, U.S. Army LABCOM, ATTN: SLCET-EF, Ft. Monmouth, NJ 07703-5601; R. Michael Garvey, Frequency & Time Systems, Inc., 34 Tozer Road, Beverly, MA 01915; William J. Riley, EG&G, Inc., 35 Congress Street, Salem, MA 01775; Robert C. Smythe, Piezo Technology, Inc., 2525 Shader Road, P.O. Box 547859, Orlando, FL 32854-7859; and Rolf D. Weglein, 6317 Drexel Ave., Los Angeles, CA 90048.

Table of Contents

Figures

Tables

Acceleration Effects on Precision Frequency Sources

I. Description of the Phenomenon

A. General

Precision frequency sources, both quartz and atomic, are affected by acceleration. The magnitude of a quartz crystal oscillator's acceleration-induced frequency shift is proportional to the magnitude of the acceleration, it also depends on the direction of the acceleration, and on the acceleration sensitivity of the oscillator. It has been shown, empirically, that the acceleration sensitivity of a quartz crystal oscillator is a vector quantity [1]. Therefore, the frequency during acceleration can be written as a function of the scalar product of two vectors

$$f(\vec{a}) = f_o(1 + \vec{\Gamma} \cdot \vec{a}) \tag{1}$$

where $f(\vec{a})$ is the resonant frequency of the oscillator experiencing acceleration $\vec{a}$, f_o is the frequency with no acceleration (often called the "carrier frequency"), and $\vec{\Gamma}$ is the acceleration-sensitivity vector of the oscillator. The frequency of an accelerating oscillator is a maximum when the acceleration is parallel to the acceleration-sensitivity vector. The frequency shift, $f(\vec{a}) - f_o = \Delta f$, is zero for any acceleration in the plane normal to the acceleration-sensitivity vector, and it is negative when the acceleration is antiparallel to the acceleration-sensitivity vector. The frequency change due to acceleration is usually expressed as a normalized frequency change, where, it follows from Equation (1) that

$$\frac{\Delta f}{f_o} = \vec{\Gamma} \cdot \vec{a} \,. \tag{2}$$

Typical values of $|\vec{\Gamma}|$ for precision crystal oscillators are in the range of 10^{-9} per g to 10^{-10} per g. $|\vec{\Gamma}|$ is independent of acceleration amplitude for the commonly encountered acceleration levels (i.e., at least up to 20g); however, high acceleration levels can result in changes in the crystal unit (e.g., in the mounting structure) that can lead to $\vec{\Gamma}$ being a function of acceleration. $\vec{\Gamma}$ can also be a function of temperature [2].

In an atomic frequency standard, the frequency of a voltage controlled crystal oscillator (VCXO) is multiplied and locked to the frequency of an atomic resonator. The effects of acceleration on atomic standards can be divided into crystal oscillator effects, atomic resonator effects, and servo loop effects. The extent to which an acceleration-induced VCXO frequency shift affects the output frequency of the atomic standard depends on the rate of change of acceleration relative to the atomic resonator-to-crystal oscillator servo loop time constant, t_o. Fast acceleration changes ($f_{vib} >> 1/2\pi t_o$) will cause the atomic standard's acceleration sensitivity to be that of the VCXO, since the servo loop

will not be fast enough to correct the VCXO. Slow acceleration changes ($f_{vib}<<1/2\pi t_o$) will have little effect on the output frequency to the extent that the servo loop gain is sufficient to correct the VCXO frequency to that of the atomic resonator. However, it has been observed that a constant frequency offset may appear in the case where the atomic standard is submitted to a periodic vibration, even if its frequency is lower than $1/2\pi t_o$. As is shown in Appendix A, this is a servo loop effect and it occurs when the acceleration induced frequency change shows a distortion, with a component at twice the acceleration frequency in addition to that at the fundamental vibration frequency. In the case $f_{vib}<<1/2\pi t_o$, the spurious constant frequency offset is very efficiently attenuated when the value of t_o is decreased.

In general, vibration near[1] the servo loop modulation frequency, f_{mod}, (or near multiples or submultiples of f_{mod}) can cause significant frequency offsets in passive atomic frequency standards if the mechanical structure produces responses at harmonics of the vibration frequency. In the case of rubidium frequency standards, vibration of the physics package at f_{mod} can modulate the light beam, producing a spurious signal that can confuse the servo system and, thereby, cause a frequency offset (in a manner identical to that for cesium standards described below). Vibration of the VCXO at even multiples of f_{mod} produces sidebands on the microwave excitation to the Rb physics package that causes a frequency offset via an intermodulation effect [3-8]. A loss of microwave excitation power can occur at low vibration frequencies, as is shown in an example in Appendix B, section D.

At low acceleration levels, properly designed atomic resonators possess very low acceleration sensitivities; however, high acceleration levels (e.g., > 10g) can produce significant effects. For example, in a rubidium standard [3,4], the acceleration can change the location of the molten Rb inside the Rb lamp, and it can cause mechanical changes which result in deflection of the light beam. Both effects can result in a change in light and signal output, that, due to light shift and servo offset mechanisms, can cause a frequency shift. Mechanical damage can cause rf power changes that, due to the rf power shift effect, can cause a frequency shift.

In a cesium standard [8,9], high acceleration levels can affect the accuracy and stability of the output frequency through mechanisms which modify the position of the atomic trajectory with respect to the tube structure. This is most serious when the vibration frequency is near the servo modulation frequency. The vibration modulates the amplitude of the detected beam signal. The net effect of this phenomenon is normally of no consequence due to the fact that the perturbing vibration must be at or very near the servo modulation frequency and must be stable in frequency as well. When the acceleration is very near the servo modulation frequency, the vibration induced amplitude perturbation of the detected beam can be synchronously detected, leading to large output

[1] i.e., within the servo loop bandwidth.

frequency errors. It should be noted that this problem is of minimal concern in actual applications due to the requirements on the precision and stability of the frequency of the perturbing acceleration.

A more subtle problem arises from the effects on the position of the beam with respect to the microwave interrogating cavity via distributed cavity phase shift effects. Another subtle effect arises from the potential to modify the detected velocity distribution. The magnitude of these effects is small when compared to the vibration induced amplitude modulation perturbations described above.

Acceleration effects can also cause frequency offsets in cesium frequency standards via degradation of the amplitude of the interrogating microwave signal. This can happen as a result of detuning of the frequency multipliers. Good mechanical design and thorough qualification of the design will minimize problems in this area.

In hydrogen masers, the most acceleration-sensitive part is the microwave cavity [10]. A deformation of the cavity structure causes a shift of the cavity resonant frequency. This induces a change of the maser frequency via the cavity pulling effect. A cavity autotuning system is able to suppress this effect if the acceleration change is sufficiently smaller than $1/2\pi t_0$, where t_0 is the cavity servo loop time constant.

B. Types of Acceleration Effects

1. Steady-State Acceleration

When an oscillator is subjected to steady-state acceleration, the normalized frequency shifts by $\vec{\Gamma} \cdot \vec{a}$, per Equation (2). Steady-state acceleration occurs, for example, during the launching of a rocket, in an orbiting satellite, in a centrifuge, and in a gravitational field.

2. Gravity Change Effects

The frequency shift described in Equation (2) is also induced by the acceleration due to gravity. One manifestation occurs when an oscillator is turned upside down (on earth). This is commonly referred to as "2g-tipover." During 2g-tipover, the magnitude of the gravity field is 1g in the direction towards the center of the earth.[2] As is discussed in Appendix C, use of Equations 1 and 2 for gravitational field effects necessitates defining the acceleration of gravity as pointing away from the center of the earth so that the direction of $\vec{\Gamma}$ is consistent with the direction one obtains for conventional acceleration.

When an oscillator is rotated 180° about a horizontal axis, the scalar product of the gravitational field and the unit vector normal to the initial "top" of the oscillator changes

---

[2] The magnitude of acceleration is in units of g, i.e., the magnitude of the earth's gravitational acceleration at sea level, 980 cm/sec^2.

from -1g to +1g, i.e., by 2g. Figure 1 shows actual data of the fractional frequency shifts of an oscillator when the oscillator was rotated about three mutually perpendicular axes in the earth's gravitational field. For each curve, the axis of rotation was horizontal. The sinusoidal shape of each curve is a consequence of the scalar product being proportional to the cosine of the angle between the acceleration-sensitivity vector and the acceleration due to gravity, as is explained in more detail in Appendix C.

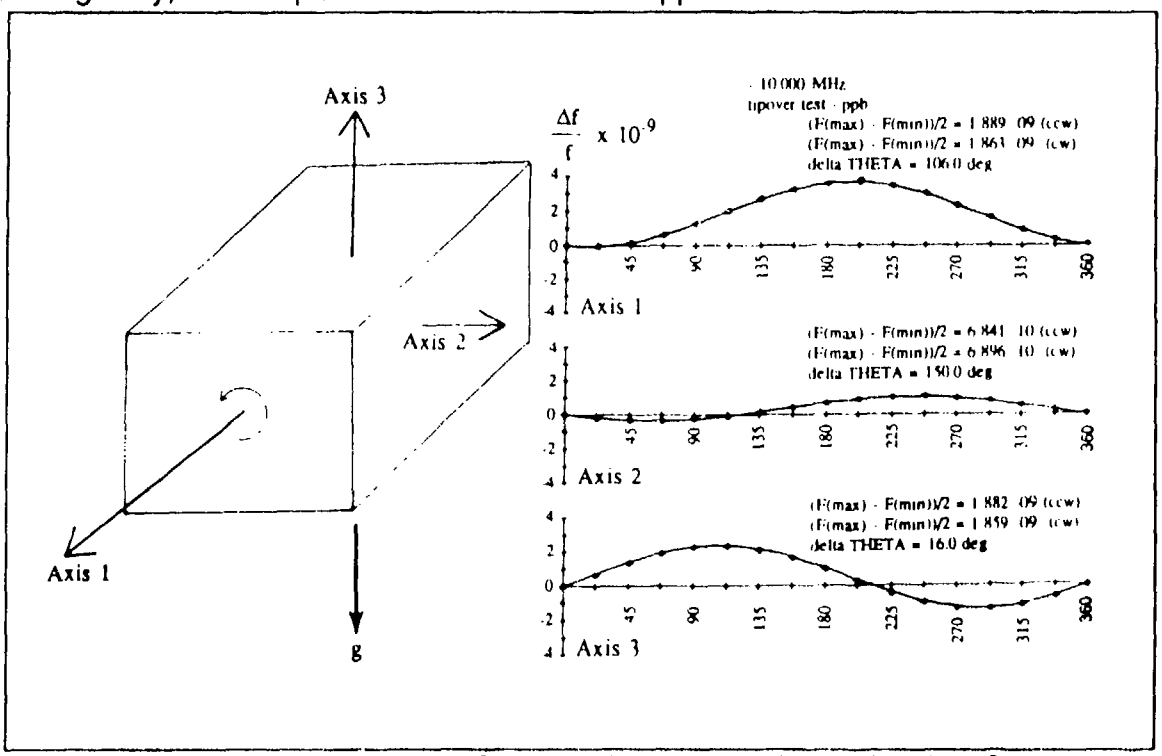

Fig. 1. "2-g Tipover," Frequency Change Versus Rotation in Earth's Gravitational Field for Three Mutually Perpendicular Axes.

Another type of gravity change effect occurs when, for example, a spacecraft containing an oscillator is sent into space. The oscillator's frequency will, again, change in accordance with Equation (1).

3. Vibration Effects

The effects of vibration on frequency stability are reviewed in Appendix B and by Filler [1]. The effects can be summarized as follows:

a. Sinusoidal Vibration

As is shown in Appendix B, for a small modulation index, $\beta = \Delta f/f_v = (\vec{\Gamma} \cdot \vec{A})f_0/f_v < 0.1$, sinusoidal vibration produces spectral lines at $\pm f_v$ from the carrier, where f_v is the vibration frequency:

$$\mathcal{L}'(f_v) = 20 \log \frac{(\vec{\Gamma} \bullet \vec{A} f_o)}{2 f_v}. \quad (3)$$

(NOTE: *$\mathcal{L}'(f)$ are spectral lines (i.e., delta functions) not spectral densities.*) Most of the power is in the carrier, a small amount is in the first spectral line pair, and the higher order spectral lines are negligible. Appendix B contains an example calculation of sinusoidal vibration-induced spectral lines.

b. Random Vibration

For a small modulation index, random vibration's contribution to phase noise is given by:

$$\mathcal{L}(f) = 20 \log \left(\frac{\vec{\Gamma} \bullet \vec{A} f_o}{2 f} \right), \quad (4)$$

where $|\vec{A}| = [(2)(PSD)]^{1/2}$ and PSD is the power spectral density of the vibration. The use of $\mathcal{L}(f)$ is in conformance with IEEE-1139-1988 [11]. Appendix B contains example calculations. As can be seen from the examples, vibrating platforms can cause severe phase noise degradation.

Not only does random vibration degrade the spectrum, but the time errors due to random vibration also accumulate. The time (or phase) errors do not average out because the white frequency noise is integrated to produce random walk of the phase. The noise of an oscillator produces time prediction errors of $\sim \tau \sigma_y(\tau)$ for prediction intervals of τ [12].

c. Acoustic Noise

MIL-STD-810D describes the effects of acoustic noise as follows: "Acoustic noise can produce vibration in equipment similar to that produced by mechanically transmitted vibration. In an acoustic noise field, pressure fluctuations impinge directly on the equipment. The attenuation effects of mechanical transmission are missing and the response of the equipment can be significantly greater. Further, components which are effectively isolated from mechanical transmission will be excited directly. Examples of acoustically induced problems:

a. Failure of microelectronic component lead wires.
b. Chafing of wires.
c. Cracking of printed circuit boards..."

In addition to these problems, the response of an oscillator to acoustic-noise-induced acceleration is the same as the response to any other type of vibration, i.e., the acoustic

noise modulates the oscillator's frequency [13]. The modulation (or phase noise degradation) is a function of the acoustic-noise-induced vibration's amplitudes, directions, and frequencies.

Acoustic noise can have a broad spectrum. For example, in a missile environment, it may extend to frequencies above 50 kHz. An effect of such noise, e.g., in 100 MHz 5th overtone resonators, may be the excitation of flexural modes (microphonics) in the crystal plate [14]. These flexural modes in turn can produce undesirable spectral lines in the phase noise spectrum. The magnitudes of these lines are independent of the resonator's $\vec{\Gamma}$ and depend chiefly on the plate geometry and mounting structure.

Acoustic noise can be especially troublesome in certain applications. For example, when an extremely low noise oscillator was required in an aircraft radar application, after the system designers built a three-level vibration isolation system to isolate the oscillator from the vibration of the aircraft, they discovered that the isolation system failed to deliver the expected phase noise of the oscillator because the isolation system failed to deal with the acoustic noise in the aircraft; i.e., the isolation system was effective in isolating the oscillator from the vibrations of the airframe, but it was ineffective in blocking the intense sound waves that impinged on the oscillator.

d. Oscillator Sustaining Stage Vibration

When a crystal oscillator is subjected to vibration, the primary cause of the resultant output signal frequency modulation is the acceleration sensitivity of the quartz crystal resonator. However, vibration-induced mechanical motion in other circuit components, and in the circuit board itself, can also result in output signal frequency and/or phase modulation. In general, these effects are more pronounced in higher frequency (i.e., VHF) oscillators due to a combination of: (1) increased circuit signal phase sensitivity to mechanical motion (i.e., increased phase shift for a given amount of circuit reactance variation due to a larger resonator C_1), and (2) decreased crystal resonator Q.

If the vibration-induced circuit phase shift occurs inside the oscillator feedback loop, there will be a conversion of phase-to-frequency modulation for vibration frequencies within the resonator half-bandwidth. The phase-to-frequency conversion is related to the resonator group delay (i.e., loaded Q). For vibration frequencies in excess of the resonator half-bandwidth, the vibration-induced phase modulation sidebands may or may not be further attenuated, depending on whether or not the induced modulation is occurring in a portion of the circuit signal path which is subject to resonator frequency selectivity.

Methods for minimizing these effects include use of multiple circuit board chassis mounting points, circuit potting, wire and cable tie down, elimination of adjustable components or post-tuning cementing in place of adjustors, avoidance of non-potted and non-shielded inductors, and avoidance of very high circuit nodal impedances that are

sensitive to nodal capacitance variation. As an example, measurements on a 100 MHz SC-cut crystal oscillator indicate that, when these precautions are taken, sustaining stage carrier signal phase shift sensitivity to vibration on the order of 10^{-6} radians per g can typically be obtained. This represents a situation where sustaining stage vibration-induced signal phase modulation becomes dominant (as compared to resonator frequency modulation effects) only at vibration frequencies in excess of approximately 50 kHz.

e. Frequency Multiplication

Upon frequency multiplication by a factor N, the vibration frequency f_v is unaffected since it is an external influence. The peak frequency change due to vibration, Δf, however, becomes

$$\Delta f = (\vec{\Gamma} \cdot \vec{A})\, N f_o . \tag{5}$$

The modulation index β is therefore increased by the factor N. Expressed in decibels, frequency multiplication by a factor N increases the phase noise by 20 log N.

When exposed to the same vibration, the relationship between the vibration-induced phase noise of two oscillators with the same vibration sensitivity and different carrier frequencies is

$$\mathcal{L}_B(f) = \mathcal{L}_A(f) + 20 \log (f_B / f_A) , \tag{6}$$

where $\mathcal{L}_A(f)$ is the sideband level, in dBc/Hz (or dBc for sinusoidal vibration), of the oscillator at frequency f_A, and $\mathcal{L}_B(f)$ is the sideband level of the oscillator at frequency f_B. For the same acceleration sensitivity, vibration frequency and output frequency, the sidebands are identical, whether the output frequency is obtained by multiplication from a lower frequency or by direct generation at the higher frequency. For example, when a 2 x 10^{-9}/g sensitivity 5.0 MHz oscillator's frequency is multiplied by a factor of 315 to generate a frequency of 1575 MHz, its output will contain vibration-induced sidebands which are identical to those of a 1575 MHz SAW oscillator which has the same 2 x 10^{-9}/g sensitivity.

f. Large Modulation Index

A large modulation index, i.e., $\beta > 0.1$, can occur in UHF and higher frequency systems, and at low vibration frequencies. When the modulation index is large, it is possible for the sidebands to be larger than the carrier. At the values of β where $J_o(\beta) = 0$, e.g., at $\beta = 2.4$, the sidebands-to-carrier power ratio goes to infinity (see equation (B.9) in Appendix B), which means that all of the power is in the sidebands, none is in the carrier. Such "carrier collapse" can produce catastrophic problems in some applications. See Appendix B for large modulation index examples.

g. Two-Sample Deviation

The two-sample deviation [11] (or square-root of the Allan variance) $\sigma_y(\tau)$ is degraded by vibration because the vibration modulates the oscillator's output frequency. The typical degradation due to sinusoidal vibration varies with averaging time, as shown in Figure 2. Since a full sine wave averages to zero, the degradation is zero for averaging times that are integer multiples of the period of vibration. The peaks occur at averaging times that are odd multiples of half the period of vibration. The $\sigma_y(\tau)$ due to a single-frequency vibration is:

$$\sigma_y(\tau) = \frac{\vec{\Gamma} \cdot \vec{a}}{\pi} \frac{\tau_v}{\tau} \sin^2(\pi \frac{\tau}{\tau_v}), \qquad (7)$$

where τ_v is the period of vibration, τ is the measurement averaging time, $\vec{\Gamma}$ is the acceleration sensitivity vector, and $\vec{a}$ is the acceleration.

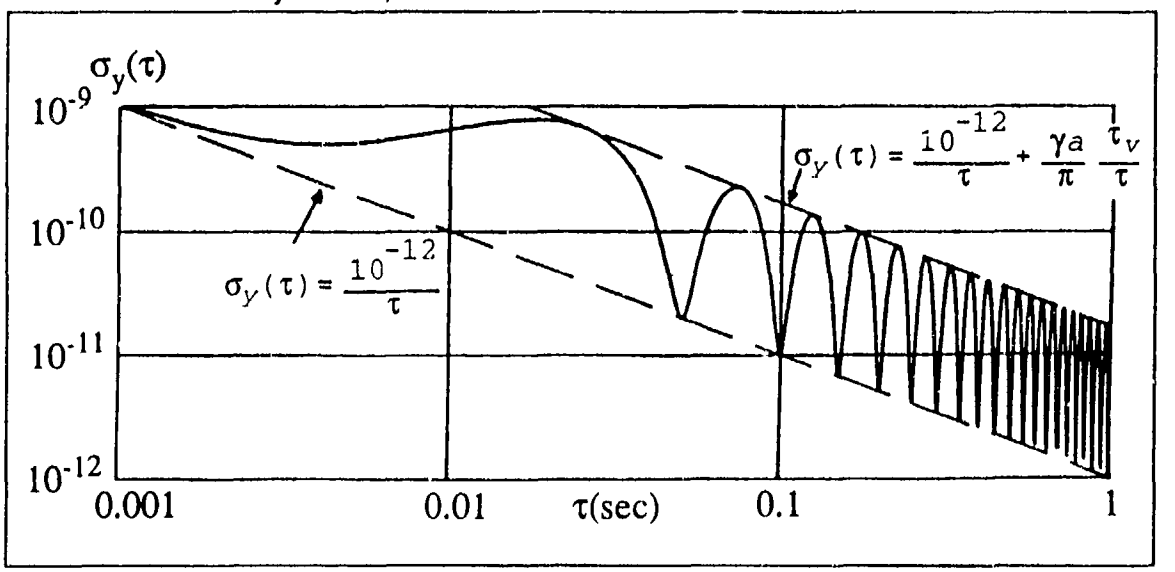

Fig. 2. Vibration-Induced Allan Variance Degradation Example (f_v = 20 Hz, |a| = 1.0g, $|\vec{\Gamma}| = 1 \times 10^{-9}$/g).

h. Integrated Phase Noise, Phase Excursions, Jitter and Wander

Specialists in crystal resonators and oscillators generally characterize phase noise by $S_\phi(f)$ or $\mathcal{L}(f)$ [11]. Many users of crystal oscillators, however, characterize phase noise in terms of "phase jitter."

In digital communications, the terms jitter and wander are used in characterizing timing instabilities. Jitter refers to the high-frequency timing variations of a digital signal and wander refers to the low-frequency variations. The dividing line between the two is

often taken to be 10 Hz. Wander and jitter, whether caused by vibration or otherwise, can be characterized by the appropriate measurement of the RMS time error of the clock. A 10 Hz low pass filter should be used to remove the effects of jitter if necessary. For very high Fourier frequencies or short integration times, it may be necessary to calculate the jitter from the spectrum rather than to measure it directly. For example, the mean-square phase jitter during a one-tenth second interval is the integral of the phase instability $S_\phi(f)$ over the Fourier frequency range from 10 Hz to infinity [12].

The integrated phase noise for the bandwidth f_1 to f_2 is

$$\Delta\phi_i^2 = \int_{f_1}^{f_2} S_\phi(f)\,df. \tag{8}$$

For random vibration, it can be shown that

$$S_\phi(f) = \frac{1}{2f_v^2}(PSD)(|\vec{\Gamma}|\,f_o)^2. \tag{9}$$

When the oscillator is subjected to a simple sinusoidal vibration, the peak phase excursion follows from Equation (B.6), i.e.,

$$\Delta\phi_{peak} = \Delta f / f_v. \tag{10}$$

In a phase-locked-loop, for example, the magnitude of the phase excursion determines whether or not the loop will break lock under vibration. For example, if a 10 MHz, 1 x 10^{-9}/g oscillator is subjected to a 10 Hz sinusoidal vibration of amplitude 1 g, the peak vibration-induced phase excursion is 1 x 10^{-3} radians. If this oscillator is used as the reference oscillator in a 10 GHz radar system, the peak phase excursion at 10 GHz will be 1 radian. Such a large phase excursion can be catastrophic to the performance of many systems, such as those which employ phase-locked-loops (PLL) or phase shift keying (PSK).

i. Spectral Responses at Other than the Vibration Frequency

Spectral responses at other than the vibration frequency may arise from a nominally sinusoidal vibration source of frequency f_v, if the source is not a pure sinusoid [14]. This usually occurs when the source is driven hard to generate vibration near its maximum output power, so that it operates in the nonlinear regime. Under these circumstances, the spectrum of the vibration source itself will contain not only the spectral line at frequency f_v but also lines at harmonic frequencies, $2f_v$, $3f_v$, etc. A spectrum check of the vibration source is recommended in such cases.

Even if the vibration source is a pure sinusoid at frequency f_v, it is still possible to excite oscillator vibration responses at harmonically related vibration frequencies $2f_v$, $3f_v$, etc. if the vibration level is excessive so as to drive materials in the oscillator into the

nonlinear range. This situation is readily identified by observing the effect of reducing the vibration source amplitude.

Oscillator spectral responses at other than the vibration frequency have also been observed in cases where the oscillator is subjected to a random vibration spectrum. These responses are excited at frequencies much higher than the exciting spectrum and are the result of nonlinear phenomena in the crystal plate and/or the oscillator. The responses are in the form of spectral lines at carrier offset frequencies that correspond to the flexural modes of the crystal plate. The flexural mode frequencies are determined, in decreasing order of importance, by the number of crystal plate support posts, by the plate thickness and by the crystal cut. For example, the typical spectral response range in a 100 MHz, 4-post supported crystal plate extends upward from 12.2 kHz, the fundamental mode flexural frequency [14]. It has been observed that these responses are minimized in a crystal plate that is compliantly supported rather than hard mounted.

4. Shock Effects

When a crystal oscillator experiences a shock, frequency (and phase) excursions result which, in a properly designed oscillator, are due primarily to the quartz resonator's stress sensitivity. The magnitude of the excursion is a function of resonator design, and of the shock-induced stresses on the resonator. (Resonances in the mounting structure will amplify the stresses.) A permanent frequency offset usually results which can be due to: shock-induced stress changes (when some elastic limits in the resonator structure are exceeded), the removal of (particulate) contamination from the resonator surfaces, and changes in the oscillator circuitry, e.g., due to changes in stray capacitances.

The shock-produced phase excursions can be calculated from Equations (B.1) and (B.5), with the proviso that at high acceleration levels, $\vec{\Gamma}$ may be a function of $\vec{a}$. For example, for a half-sine shock pulse of duration D

$$\Delta\phi_{peak} = 2 D f_o \vec{\Gamma} \cdot \vec{a} . \qquad (11)$$

Upon frequency multiplication by N, the $\Delta\phi_{peak}$ becomes N times larger, so in systems where the frequency is multiplied to microwave (or higher) frequencies, the shock-induced phase excursion can cause serious problems, such as loss of lock in PLL systems, and bit errors in PSK systems.

Survival under shock (and under vibration) is primarily a function of resonator surface imperfections. Even minute scratches on the surfaces of the quartz plate result in orders of magnitude reductions in the resonator's shock resistance [15]. Chemical-polishing-produced scratch-free resonators have survived shocks of up to 36,000g in air gun tests, and have survived the shocks due to being fired from a 155mm howitzer (16,000g, 12ms duration) [16].

In atomic frequency standards, a shock-induced phase excursion of the VCXO can result in a transitory loss of lock, however, this is not a problem when the shock duration is smaller than the servo loop time constant, which is often the case. When a loss of lock does occur, the recovery time is a function of the servo loop time constant. The phase excursions of the VCXO, and of the output crystal filter, can have a significant effect on the clock output, which can disturb the host system. Shock-induced mechanical damage can cause changes (e.g., light and rf power changes in Rb standards) that can produce a permanent frequency offset. For atomic standards employing Ramsey interrogation, large (2×10^{-8}) shock-induced permanent frequency shifts of the VCXO can cause false lock acquisition to the satellite peaks in the Ramsey resonance.

5. Acceleration Effects in Crystal Filters

Some frequency sources, such as synthesizers, atomic frequency standards, and precision crystal oscillators with post-filters, contain crystal filters. In these applications they are often called spectrum cleanup filters; however, under vibration such filters modulate the signals passing through them, adding as well as removing vibration-related sidebands. Hence, spectrum cleanup filters must be used with great care in systems subject to vibration.

It is well known that the principal vibration effect in crystal filters is phase modulation, although some amplitude modulation may also occur [17,18]. Appendix D contains a further discussion and examples of calculated results for the total vibration-induced phase modulation of frequency source with post-filters.

II. Specifications

Acceleration sensitivity can be specified several ways. The appropriate specification method depends on the application and on the types of accelerations that can be expected to adversely influence the oscillator's performance. The general military specification for crystal oscillators [19], MIL-O-55310, attempts to address all aspects of acceleration sensitivity. The paragraphs dealing with acceleration sensitivity are reproduced in Appendix E. Although MIL-O-55310 was written for crystal oscillators, because the output frequencies of atomic frequency standards originate from crystal oscillators, and because no comparable document exists that addresses atomic standards specifically, MIL-O-55310 can also serve as a suitable guide to specifying atomic standards.

III. Test Methods

A. 2-g Tipover Test

In the past, the 2-g tipover test has often been used by manufacturers (and researchers) to characterize oscillators' acceleration sensitivity. This test method is deceptively simple because if not used carefully, it can yield false and misleading results.

The simple 2-g tipover test consists of measuring the frequency changes when an oscillator is turned upside down three times, about three mutually perpendicular axes. The magnitude of the acceleration sensitivity is then the vector sum (square-root of the sum of the squares) of the three frequency changes per g (where, for each axis, the frequency change per g is one-half of the measured frequency change).

There are some serious problems with using the 2-g tipover test: 1) the test is applicable only to high quality oven-controlled oscillators because in non-temperature-controlled oscillators, the frequency-shifts due to ambient temperature changes will exceed the acceleration-induced frequency changes, and, thereby, make the test results worthless; 2) many oven-controlled oscillators are not suitable for characterization by the 2-g tipover test, because rotation of the oscillator results in temperature changes (due to air convection) inside the oven that can mask the effects due to acceleration changes; similarly, in atomic standards, changes in internal thermal distribution resulting from the tipover will mask acceleration effects; 3) the results are poor indicators of performance under vibration when the vibration frequencies of interest include resonances (see section IV); 4) since magnetic fields can change the frequencies of crystal oscillators ~ 10^{-11} to 10^{-10} per gauss [20], rotation in the earth's magnetic field can produce significant errors while measuring (unshielded) low-acceleration-sensitivity crystal oscillators; and 5) in atomic frequency standards, effects of the earth's magnetic field can dominate the results, and for the reasons discussed above, the results will be irrelevant to the performance under vibration if during 2-g tipover testing the acceleration changes with a time constant that is larger than the servo-loop time constant.

A 2-g tipover test that is far more reliable than the simple test described above consists of measuring the fractional frequency changes corresponding to small changes in orientation with respect to the earth's gravitational field, e.g., as shown in Figure 1. The oscillator is first rotated, e.g., in 22.5° increments, 360° about an axis (which is usually one of the major axes of the oscillator). From the frequency changes during this rotation, one can determine two out of the three components of $\vec{\Gamma}$ (keeping in mind that $\vec{a} = -\vec{g}$ in Equations 1 and 2, as is discussed in Appendix C). The oscillator is then similarly rotated 360° about a second axis that is perpendicular to the first. From the frequency changes during this second rotation, one can determine the third component of $\vec{\Gamma}$, and, simultaneously, obtain a self-consistency check for one of the other two components (i.e., the one that is normal to both the first and second axes of rotation). The calculation details are shown in Appendix C, where it is also shown that the

frequency change vs. orientation, $\Delta f(\theta)$ vs. θ, is a sinusoidal function. The frequency changes during rotation about the third axis can provide additional self-consistency checks for the two components of $\vec{\Gamma}$ that are normal to the third axis. If the measurements are not self-consistent, and if there are large deviations in the $\Delta f(\theta)$ vs. θ from the best fit to a sinusoidal function, as will generally be the case if, for example, the resonator's temperature changes during the test, then the 2-g tipover test result is unreliable. It should be noted that, in this 2-g tipover test too, the earth's magnetic field can produce significant errors if the oscillator is unshielded and if the oscillator possesses low acceleration sensitivity.

B. Vibration Tests

The sidebands generated by sinusoidal vibration can be used to measure the acceleration sensitivity. From Equation (3)

$$\Gamma_i = \left(\frac{2 f_v}{A_i f_o}\right) 10^{B}, \text{ where } B = \mathcal{L}'_i(f_v)/20 \tag{12}$$

and where $\vec{\Gamma}_i$ and A_i are the components of the acceleration sensitivity vector and of the acceleration, respectively, in the $\hat{i}$ direction. Measurements, along three mutually perpendicular axes are required to characterize $\vec{\Gamma}$, which becomes

$$\vec{\Gamma} = \Gamma_i \hat{i} + \Gamma_j \hat{j} + \Gamma_k \hat{k} \tag{13}$$

with a magnitude of

$$|\vec{\Gamma}| = (\Gamma_i^2 + \Gamma_j^2 + \Gamma_k^2)^{1/2}. \tag{14}$$

One scheme for measuring $\vec{\Gamma}$ is shown in Figure 3. The local oscillator is used to mix the carrier frequency down to the range of the spectrum analyzer. If the local oscillator is not modulated, the relative sideband levels are unchanged by mixing. The frequency multiplier is used to overcome dynamic range limitations of the spectrum analyzer, using the "20 log N" enhancement discussed previously. The measured sideband levels must be adjusted for the multiplication factor prior to insertion into Equation (12). It must be stressed that Equation (12) is valid only if $\beta < 0.1$. A sample measurement output and calculation is shown in Figure 4.

In order to detect frequency sensitivities, e.g., due to vibration resonances, the sideband levels need to be measured at multiple vibration frequencies - e.g., see paragraph 4.9.38.2 of MIL-O-55310C in Appendix E. An alternative to using a series of vibration frequencies is to use random vibration, e.g., as described by D. J. Healy, III, et al. [21].

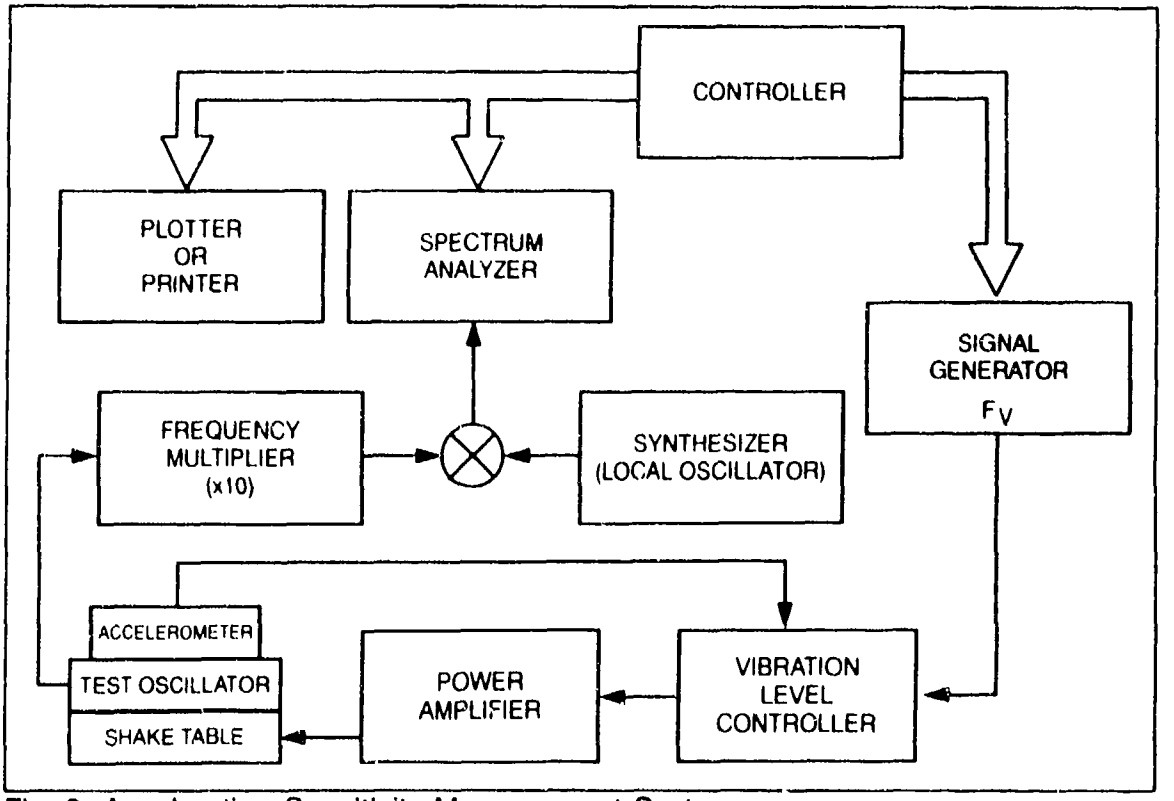

Fig. 3. Acceleration Sensitivity Measurement System.

Refinements of the vibration-induced-sideband method of measuring acceleration sensitivity have been described by M. M. Driscoll [22], and by M. H. Watts, et al. [23]. Driscoll's method provides for minimization of measurement errors due to cable vibration. The method also allows measurement of acceleration sensitivity of the resonator alone. The resonator is mounted on the shake table and is connected to the oscillator circuitry via a quarter wavelength cable. The oscillator circuitry remains at rest while the resonator is vibrated.

In the result of the vibration-induced-sideband method of measuring acceleration sensitivity, there is a 180° ambiguity in the direction of $\vec{\Gamma}$, i.e., the results cannot distinguish between two oscillators, the $\vec{\Gamma}$'s of which are antiparallel. In the method of Watts, et al., the sensitivity of doubly rotated quartz resonators to voltages applied to the electrodes is used to resolve the ambiguity. When the proper magnitude applied voltage is in-phase with the applied acceleration, the sidebands are increased. When the applied voltage is 180° out of phase with the acceleration, the sidebands are decreased. The method allows not only the determination of the sign of $\vec{\Gamma}$, but also the elimination of cable vibration effects.

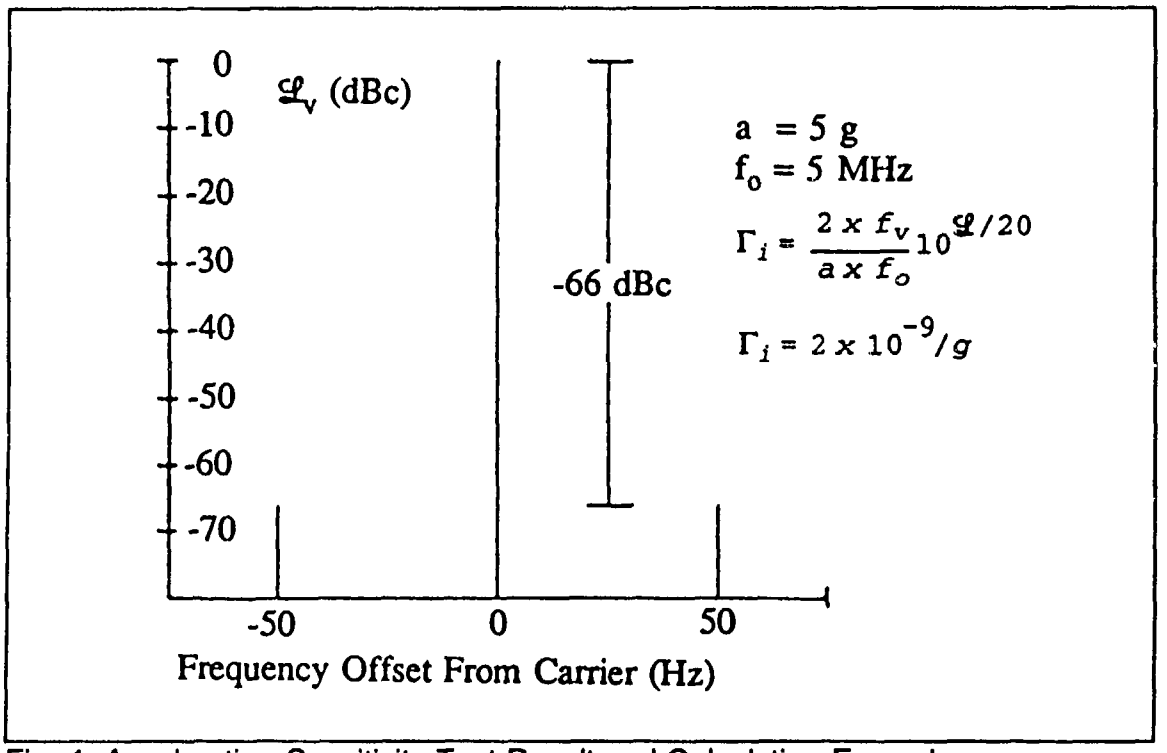

Fig. 4. Acceleration Sensitivity Test Result and Calculation Example.

C. Shock Tests

The shock testing of a frequency source generally consists of measuring the frequency or phase of the source before and after exposing the device to the specified shock. The phase deviation resulting from the shock (which is the time integral of the fractional frequency change) can provide useful information about the frequency excursion during the shock (including the possible cessation of operation).

D. Safety Issues

During acceleration sensitivity testing, one must ensure both the operator's and the equipment's safety. Exposing the operator to high intensity noise may cause permanent hearing loss. In the U.S.A., OSHA [24] regulations require employers to provide protection against the effects of high noise exposures, and to administer "a continuing and effective hearing conservation program," whenever the noise exposures exceed specified levels. The permissible noise exposures are functions of both the sound levels and the exposure durations.

For both the operator's and the equipment's safety, all parts subjected to testing must be securely fastened. The forces generated during vibration testing can be high enough to shear the bolts that hold down the equipment.

IV. Interactions and Pitfalls

The two major influences that can interact with the effects of acceleration during testing are thermal effects and magnetic field effects. If the oscillator's temperature changes during acceleration-sensitivity testing, then the temperature-induced frequency shifts can interfere with measurement of the acceleration-induced frequency shifts, as is discussed above in the "2-g Tipover Test" section, for example. Another example of interference by thermal effects is the cooling due to increased air flow during testing in a centrifuge.

Similarly, ac magnetic fields can produce sidebands which can interfere with the vibration-induced sidebands, and dc magnetic fields can produce frequency offsets in atomic frequency standards. Two sources of magnetic fields are the earth's field, and coils in shake-tables and centrifuges. Induced ac voltages due to motion in the earth's magnetic field and due to magnetic fields of the shake table can affect, e.g., varactors, AGC circuits, and power supplies. Since the frequency of a vibration-induced ac voltage is the vibration frequency, the sidebands due to ac voltages are superimposed on the vibration-induced sidebands. One solution to shake-table-produced magnetic fields is to use hydraulic shakers. Such devices are less commonly available than electrodynamic shakers, and have a lower frequency range.

Resonance phenomena can lead to other pitfalls in the determination and specification of acceleration sensitivity. Resonances can occur not only within the oscillator, but also in the test setup and in the platform where the oscillator is to be mounted. Figure 5 shows test results for an oscillator that had a resonance at 424 Hz. (The resonance was traced to a flexible circuit board within the oscillator.) The resonance amplified the acceleration sensitivity at 424 Hz by a factor of 17. It is, therefore, important to test oscillators at multiple vibration frequencies (with either a series of sinusoidal vibration frequencies or with random vibration) in order to reveal resonances. It is also important to determine the resonances in the platform where the oscillator is to be mounted, and to take that information into account during the specification of acceleration sensitivity.

The accelerometers used in vibration-sensitivity testing have non-ideal frequency responses, usually at both low (near DC) and high frequencies. The useful frequency range at the high end is limited by resonances in the accelerometer. The limitations of the accelerometer can be measured, and can also usually be obtained from the manufacturer. The limitations should be taken into account during acceleration-sensitivity testing. Similarly, the limitations of other components in the test setup, e.g., the spectrum analyzer, the signal generator and the shake table must be taken into account (e.g., the shake table may produce vibrations transverse to the intended direction). Another factor to consider is that spectral responses at other than the vibration frequency can occur, as was discussed earlier.

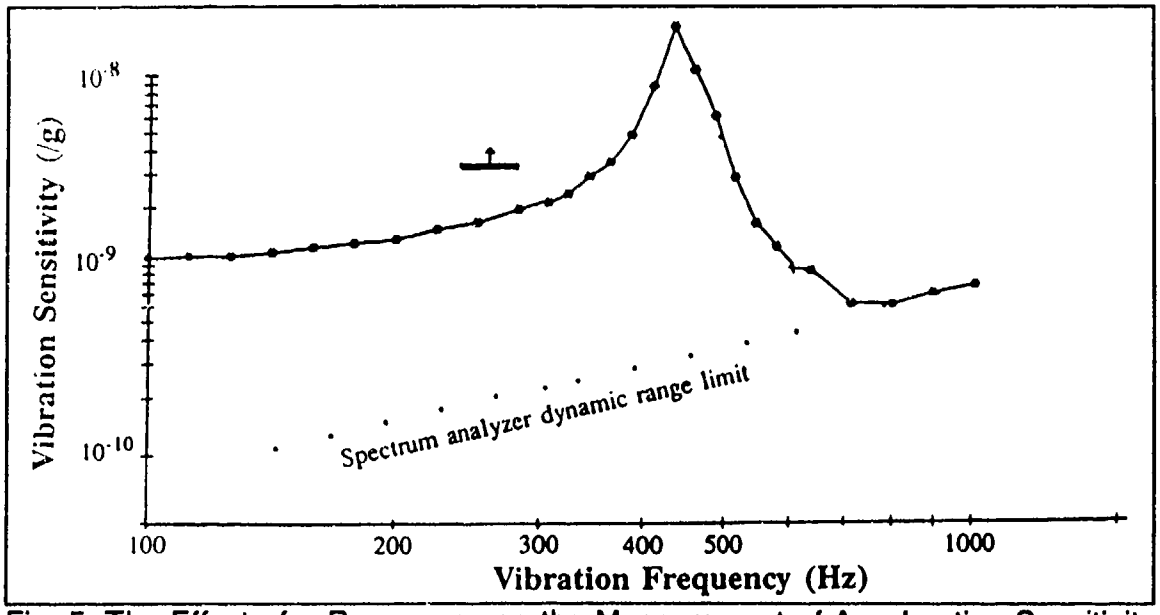

Fig. 5. The Effect of a Resonance on the Measurement of Acceleration Sensitivity vs. Vibration Frequency.

Vibration isolation has been proposed as the "fix" for the acceleration sensitivity of frequency sources. The pitfalls of using such a "fix" are: 1) isolation systems have a limited frequency range of usefulness; outside this range, the isolation systems amplify the problem; 2) a single isolator isolates the vibration primarily along a single direction; 3) isolation systems add size, weight and cost; and 4) most isolation systems are ineffective against acoustic noise. Figure 6 illustrates the frequency response of a typical passive vibration isolator. It shows that, although such a device can be effective at high frequencies, it amplifies the problem at low frequencies, in the region of the isolator's resonant frequency.

V. Acceleration Related Specifications and General References

Documents, in addition to MIL-O-55310, which are frequently called out in the specification of the acceleration sensitivity testing of frequency sources are MIL-STD-202, "Test Methods for Electronic and Electrical Component Parts," and MIL-STD-810, "Environmental Test Methods and Engineering Guidelines." Some of the acceleration-related paragraphs in these standards are used for survival tests. General information on shock and vibration testing can be found in books [25-27].

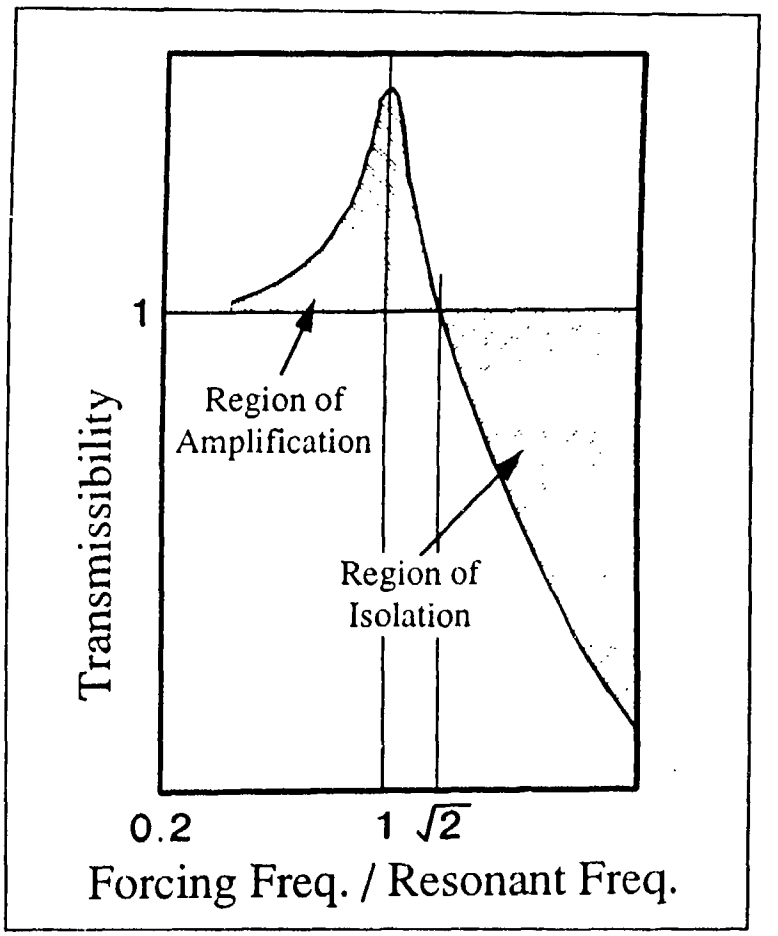

Fig. 6. Vibration Isolator Frequency Response.

Appendix A
Frequency Shift in Atomic Beam Standards due to "Rocking" (Low Frequency Sinusoidal Angular or Linear Motion)

The following analysis addresses an average frequency offset that is observed in cesium beam frequency standards caused by low frequency periodic motion. This motion can be either linear or angular in nature and for the purposes of this discussion is called rocking.

The only components of the cesium standard that are appreciably affected by rocking are the cesium beam tube and the quartz flywheel oscillator. Conventional beam tubes are sensitive to linear acceleration in the direction that is normal to both the beam and beam ribbon. The sensitivity in this direction is due to the fact that the deflection of the beam caused by the acceleration is parallel to the desired deflections produced by the state separation magnets. The beam tube consequently is also very sensitive to angular motion about an axis that is normal to the beam but in the plane of the beam ribbon. This is due to the effective acceleration associated with the Coriolis effect on the moving atoms in the beam when viewed in a coordinate system fixed to the tube. This effective acceleration is also parallel to the desired deflections. Periodic accelerations of both these types evidence themselves as amplitude modulation of the recovered signal, background modulation, and linewidth modulation. Angular rocking, as will be shown later, can lead to large effective accelerations. Also there is a $\pi/2$ shift in the phase of the effective acceleration for low angular rocking frequencies. All the phase angles are essential elements of the analysis.

The main effect on the quartz flywheel oscillator at these low frequencies is frequency modulation caused by change in orientation of the crystal with respect to the gravitational g vector due to angular rocking. This is an important effect at the present state of the technology of quartz resonators. The frequency modulation that is important in cesium beam standards is the residual modulation that remains with the standard's frequency control loop operating. At frequencies below the loop cutoff frequency, the frequency modulation of the free running oscillator is reduced and its phase is shifted by the attenuation characteristics of the servo loop.

An assumption used in this first analysis is that the intentional modulation used to find the line center is sinusoidal frequency or phase modulation at a low frequency. Then the normalized beam tube output signal under modulation and rocking but neglecting any constant background can be approximated as

$$I(t) = B(t) + \frac{1 + A(t)}{2}\left[1 + \cos\left(\frac{k\,F(t)}{1+L(t)}\right)\right] \qquad (A.1)$$

where

$k = \pi/f_L$,

f_L = static beam tube linewidth, Hz,

$F(t) = \Delta f + M \cos(m) + f1 \cos(v + \phi_{f1}) + f2 \cos(2v + \phi_{f2})$,

Δf = average frequency departure from line center, Hz,

M = peak frequency modulation of the intentional line-center-finding-modulation, Hz,

$m = \omega_m t$, where ω_m is the modulation angular frequency, radians/sec,

f1 = residual rocking peak frequency amplitude of quartz flywheel (multiplied to cesium frequency) in Hz at the rocking frequency,

f2 = residual rocking peak frequency amplitude of quartz flywheel (multiplied to cesium frequency) in Hz at second harmonic of rocking frequency,

$v = \omega_v t$, where ω_v is the rocking angular frequency,

ϕ_x = phase angles for the time responses to rocking relative to the phase of the rocking position function (this applies to either linear or angular rocking position),

$L(t) = lw \cos(v + \phi_{lw}))$, fractional dynamic beam tube linewidth modulation,

lw = peak fractional change in linewidth due to rocking,

$A(t) = a \cos(v + \phi_a)$, fractional dynamic amplitude modulation,

a = peak fractional amplitude change due to rocking,

$B(t) = b \cos(v + \phi_b)$, dynamic background signal,

b = background amplitude due to rocking,

f_o = line center frequency, Hz, and

$\omega_o = 2\pi f_o$, radians/sec.

Note that residual rocking frequency peak amplitudes, f1 and f2, are the values with the cesium servo loop operating (closed-loop values), not the free-running oscillator values. The servo loop acts as a high-pass filter that attenuates the free-running

amplitudes when the rocking frequency is below the loop cutoff frequency, 20 dB/decade for a single integrator loop and 40 dB/decade for a double integrator loop. There is also phase shift associated with the attenuation, $\pi/2$ radians for a single integrator loop and π radians for a double integrator loop when the rocking frequency is far below servo loop cutoff.

The calculation is done as follows. The servo loop of the cesium standard always forces the amplitude of the fundamental modulation frequency component of I(t) (as sensed by a synchronous detector with the modulation signal as reference) to be zero with a response time constant determined by the loop characteristics. This is accomplished by controlling the average microwave excitation frequency to the cesium beam tube. The microwave frequency is synthesized from the quartz flywheel oscillator. If the intentional modulation is distortion free, the microwave spectrum free of extraneous sidebands, and there is no rocking, then the average frequency will be at the center of the line corresponding to $\Delta f = 0$ where we have neglected the very small error due to the Bloch-Siegert effect and any error associated with the small asymmetry caused by the special relativistic effects due to the velocity spread in the beam.

To represent this behavior mathematically, I(t) is first multiplied by cos(m) to perform the synchronous detection and the result is expanded with the assumption that Δf, f1, f2, and lw are small but that M is large. It is also assumed that the frequency of the rocking is incoherent with and lower than the modulation frequency. The expansion is done to second order in f1 (for reasons to be explained later) and to first order in Δf, f2, and lw; a and b are exactly first order already. The zero frequency term, which contains all the parts that are free of periodic functions of m and/or v, is set equal to zero and the resulting equation is solved for Δf, the average frequency offset in Hz caused by the rocking. The final result is again expanded to keep only first order terms in a, b, f2, and lw and second order terms in f1.

The calculations are fairly long and tedious so we will present only the results here. The average fractional frequency offset due to the lowest order terms of the rocking effects is:

$$\frac{\Delta f}{f_o} = \frac{f1\ lw \cos(\phi_{f1} - \phi_{lw})}{2 f_o} - \frac{f1\ a \cos(\phi_{f1} - \phi_a)}{2 f_o} + \frac{f1^2\ f2\ k^2 \cos(2\phi_{f1} - \phi_{f2})}{8 f_o} \qquad \text{(A.2)}$$

Several things are apparent. The modulated background term, B(t), contributes nothing since b is absent. The two remaining tube effects, linewidth and amplitude modulations, are multiplied by f1. They can cancel if their phases are the same, that is, if $\phi_{lw} = \phi_a$. This turns out to be the case for many tube designs and the relative

amplitudes a and lw can be controlled to a fair degree, giving the capability of moderately good cancellation. Also, since the tube and crystal effects are vectorial in nature, the frequency shift can be reduced by choosing the sensitive directions to be orthogonal in the mechanical design of the whole cesium standard.

As mentioned earlier, the atomic cesium beam experiences a Coriolis effect when there is angular rocking. If the rocking frequency is very low compared with the reciprocal of the beam transit time, the effective linear acceleration of the beam tube undergoing rocking is approximately:

$$acc(t) = 2\ \theta_p\ \omega_v\ v_{beam}\ \cos(\omega_v\ t + \pi/2) \qquad (A.3)$$

when the rocking angle is

$$\theta_{rocking}(t) = \theta_p\ \cos(\omega_v\ t) \qquad (A.4)$$

where

θ_p is the peak rocking angle, radians,

v_{beam} is the velocity of the atoms in the beam, cm/sec, and

t is the time, seconds.

(Acceleration will be cm/sec^2 with the units used above.)

A reasonable value for v_{beam} in a commercial beam tube is $v_{beam} = 1.3 \times 10^4$ cm/sec. If we take $\omega_v = 0.6$ radians/sec (a rocking period of 10 seconds) and $\theta_p = 0.3$ radians (17°), we get a peak effective acceleration of about 4680 cm/sec^2 or 4.8 g. This illustrates that the Coriolis effect can easily lead to large effective accelerations.

Note the phase shift mentioned earlier of $\pi/2$ radians between the effective acceleration and the rocking angle. For linear rocking there is a phase shift of π radians between the rocking angle and the acceleration. These phase angles affect the frequency shift through the cosine factors in Equation (A.2).

The third term in Equation (A.2) is independent of the beam tube. It involves the quartz flywheel oscillator only and consequently is second order in f1 and first order in f2. This is the reason why second order terms in f1 were kept in the analysis.

The same type of analysis was done also for slow square-wave frequency modulation. The results to lowest orders are identical to those given by Equation (A.2).

To carry the analysis further requires a functional form for the servo loop frequency response of the cesium standard. We consider two cases here, a first order or single

integrator loop, and a second order or double integrator loop. The representation used here for the first order loop frequency response to oscillator frequency change is

$$f1_1 = f1_0 \frac{j\omega_v}{j\omega_v + \omega_{cl}} \qquad \text{(A.5)}$$

where

$f1_0$ is the amplitude of the free-running oscillator response to the acceleration,

$f1_1$ is the closed-loop response amplitude,

ω_v is the angular rocking frequency,

ω_{cl} is the angular cutoff frequency of the servo loop, and

$j = (-1)^{1/2}$, the square root of (-1).

This has magnitude $\omega_v/(\omega_v^2 + \omega_{cl}^2)^{1/2}$ and phase angle $\pi/2 - \tan^{-1}(\omega_v / \omega_{cl})$.

The representation for the second order loop frequency response, chosen to have two real poles in the s-plane, is

$$f1_2 = f1_0 \frac{-\omega_v^2}{-\omega_v^2 + \frac{j\,5\,\omega_v\,\omega_{cl}}{2} + \omega_{cl}^2} \qquad \text{(A.6)}$$

This has magnitude $\omega_v^2/[(\omega_v^2 - \omega_{cl}^2)^2 + 25\,\omega_v^2\,\omega_{cl}^2 / 4]^{1/2}$ and phase angle $\pi - \tan^{-1}[2.5\,\omega_v\,\omega_{cl} / (\omega_{cl}^2 - \omega_v^2)]$. Note that this phase angle goes from 0 at very high frequencies through $\pi/2$ at $\omega_v = \omega_{cl}$ to π at very low frequencies.

$f2_1$ and $f2_2$, the second harmonic amplitudes, are obtained from Equations (A.5) and (A.6) with ω_v replaced everywhere by $2\,\omega_v$ and f1 replaced by f2.

Figure A.1 shows the absolute value of the results from Equation (A.2) for angular rocking with the servo loop characteristics given above. The parameters chosen for the plot are:

ω_{cl} = 0.3 rad/sec,

peak rocking angle = 0.3 rad,

tube amplitude or linewidth sensitivity = 0.001 per g,

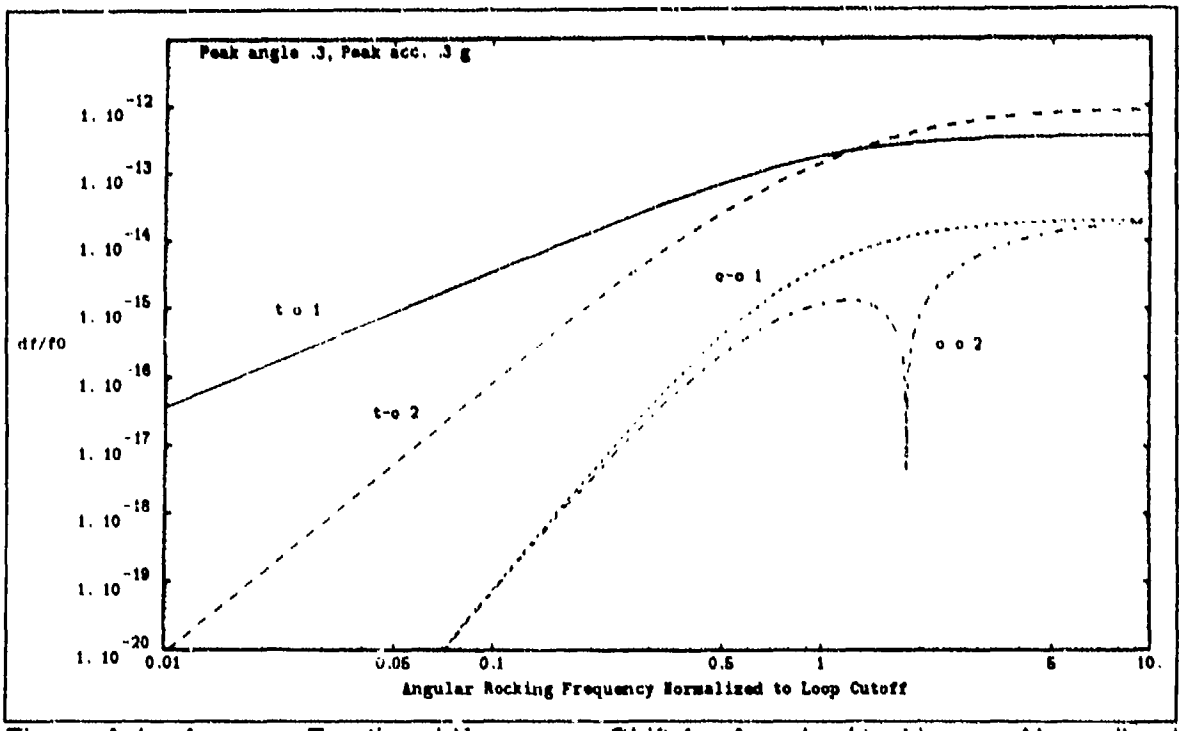

Figure A.1. Average Fractional Frequency Shift for Angular Rocking vs. Normalized Rocking Angular Frequency.

$f1_0 / f_0 = f2_0 / f_0 = 3 \times 10^{-10}$ (oscillator open-loop fractional frequency sensitivities to the rocking assuming about 1×10^{-9} per g),

f_l = 370 Hz (tube static linewidth).

The plot is for the worst cases where there is no cancellation of the beam tube sensitivities and the most sensitive axis of the tube is parallel to the most sensitive axis of the quartz crystal. The frequency axis has been normalized to the loop cutoff frequency. The curve labeled "t-o 1" is for the tube-oscillator interaction with a first order loop (first and second terms in Equation (A.2)); "t-o 2" is for the second order loop. The curve labeled "o-o 1" is for the oscillator-only sensitivities, fundamental and second harmonic (third term in Equation (A.2)); "o-o 2" is the corresponding curve for the second order loop. The null at $\omega_v / \omega_{cl} = 1.7$ is caused by the argument of the cosine in Equation (A.2) going through $\pi/2$. The sign of the shift changes on going through the null. The absolute value of the low frequency dependence of the shifts on ω_v / ω_{cl} is given in Table A.1.

Figure A.2 shows the absolute value of the results from Equation (A.2) for linear rocking. Only the tube-oscillator results are plotted since the oscillator-only results are similar to those for angular rocking except for the fact that the crystal response to the rocking is linear so that any second harmonic must be present in the rocking source. Note that the low frequency dependence for the first and second order loops is the same.

Table A.1
Low Frequency Dependence of Shifts on
ω_v / ω_{ul}.

Interaction Type in Figure A.1	Low Frequency Dependence
t-o 1	$(\omega_v / \omega_{ul})^2$
t-o 2	$(\omega_v / \omega_{ul})^4$
o-o 1	$(\omega_v / \omega_{ul})^6$
o-o 2	$(\omega_v / \omega_{ul})^6$

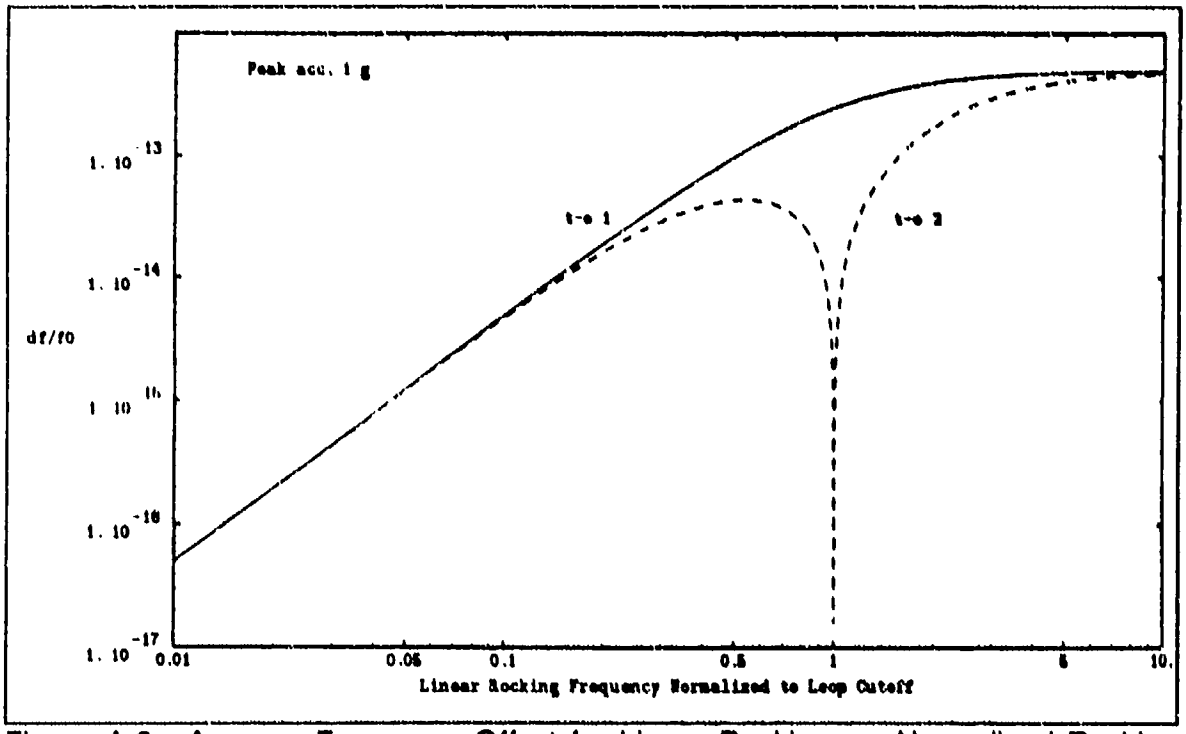

Figure A.2. Average Frequency Offset for Linear Rocking vs. Normalized Rocking Angular Frequency.

They both have $(\omega_v / \omega_u)^2$ behavior. This is due to the difference in phase of the effective accelerations for the angular versus linear rocking. Again, the null is caused by the argument of the cosine going to zero at $\omega_v / \omega_u = 1$; 1 g peak acceleration has been assumed corresponding to a peak amplitude of about 25 cm at 1 Hz rocking frequency or 25 m at 0.1 Hz. Thus, linear rocking at these low frequencies is not as important as angular rocking.

For the tube-oscillator interactions, the shift scales as (acceleration)^2. For the oscillator-only effect, the shift scales as (acceleration)^3.

It is clear that, to keep the shifts from rocking small, the loop cutoff frequency should be made as high as possible (loop time constant should be short) so that ω_v / ω_u is small.

If the amplitude and/or frequency of the angular rocking gets large the tube behavior can become very nonlinear and this analysis will no longer be valid. Putting effort into good tube design to get cancellation or compensation of the acceleration effects, along with proper care with regard to the relative orientations of the tube and oscillator, can reduce the offset by a factor of ten or more. This is important if the shifts are to be kept less than 1×10^{-13} since the worst case results can be about 1×10^{-12} for 0.3 radians peak rocking angle at a frequency several times the loop cutoff frequency.

Vibration at the modulation frequency is not covered by this calculation. The situation is more complex and depends much more on the details of the modulation. If the vibration frequency exactly equals the modulation frequency the shifts can be very large and the magnitude and sign will depend on the relative phase of the modulation and vibration. If the vibration frequency is close to the modulation frequency, there will be large frequency excursions at the difference frequency and these could drive the loop into nonlinear behavior and give an average frequency offset.

Appendix B - Vibration Effects

A. General

When an oscillator is vibrated, the time dependent acceleration changes the oscillator's output frequency in accordance with,

$$f(\vec{a}) = f_o(1 + \vec{\Gamma} \cdot \vec{a}) \tag{B.1}$$

where $\vec{a}$ is a function of time. For simple harmonic vibration, $\vec{a}$ can be expressed as

$$\vec{a} = \vec{A}\cos(2\pi f_v t) \tag{B.2}$$

where $\vec{A}$ is the peak acceleration, f_v is the vibration frequency in Hz, and t is the time in seconds. Substituting Equation (B.2) into Equation (B.1) results in

$$f(\vec{a}) = f_o + \Delta f \cos(2\pi f_v t), \tag{B.3}$$

where $\Delta f = (\vec{\Gamma} \cdot \vec{A})f_o$, i.e., the vibration modulates the output frequency by $\pm \Delta f$, at the rate f_v. The effects of vibration in the frequency domain can be seen from an examination of the output voltage of an oscillator, which can be expressed as

$$V(t) = V_o\cos(\phi(t)), \tag{B.4}$$

where the phase $\phi(t)$ is derived from the frequency by

$$\phi(t) = 2\pi \int_{t_o}^{t} f(t')\,dt'. \tag{B.5}$$

Using Equations (B.3) and (B.5), and assuming $t_o = 0$, the phase becomes

$$\phi(t) = 2\pi f_o t + (\Delta f / f_v)\sin(2\pi f_v t). \tag{B.6}$$

When Equation (B.6) is inserted into Equation (B.4), the result is

$$V(t) = V_o \cos(2\pi f_o t + (\Delta f / f_v)\sin(2\pi f_v t)). \tag{B.7}$$

Equation (B.7) is the expression for a frequency-modulated signal. It can be expanded in an infinite series of Bessel functions resulting in

$$\begin{aligned} V(t) = V_o[&J_o(\beta)\cos(2\pi f_o t) + J_1(\beta)\cos(2\pi(f_o + f_v)t) \\ &+ J_1(\beta)\cos(2\pi(f_o - f_v)t) + J_2(\beta)\cos(2\pi(f_o + 2f_v)t) \\ &+ J_2(\beta)\cos(2\pi(f_o - 2f_v)t) + \ldots] \end{aligned} \tag{B.8}$$

where $\beta = \Delta f / f_v = (\vec{\Gamma} \cdot \vec{A})f_o / f_v$ is the modulation index (from standard FM theory).

The first term in Equation (B.8) is a sine wave at the carrier frequency with an amplitude, relative to V_o, of $J_o(\beta)$. The other terms represent vibration-induced spectral

lines at frequencies $f_o + f_v$, $f_o - f_v$, $f_o + 2f_v$, $f_o - 2f_v$, etc. The ratio of the power in the nth vibration-induced spectral line to the power in the carrier, denoted by $\mathcal{L}'_n(f_v)$, is given by

$$\mathcal{L}'_n(f_v) = (J_n(\beta)/J_o(\beta))^2 \tag{B.9}$$

or, more commonly expressed in decibels as

$$\mathcal{L}'_n(f_v)(dBc) = 20 \log (J_n(\beta)/J_o(\beta)), \tag{B.10}$$

where dBc refers to dB relative to the carrier. The spectral lines $\mathcal{L}'(f_v)$ are delta functions superimposed on the phase noise spectrum $\mathcal{L}(f)$ vs. f.

In most situations, the modulation index β is less than 0.1. One can then apply the small modulation index approximation to Equation (B.10), i.e., $J_o(\beta) \cong 1$, $J_1(\beta) \cong \beta/2$, and $J_n(\beta) \cong 0$ for $n \geq 2$.

B. Sinusoidal Vibration Example

For a small modulation index, using the approximation from above, sinusoidal vibration produces spectral lines at $\pm f_v$ from the carrier, where f_v is the vibration frequency:

$$\mathcal{L}'(f_v) = 20 \log \frac{(\vec{\Gamma} \cdot \vec{A} f_o)}{2 f_v}. \tag{B.11}$$

Most of the power is in the carrier, a small amount is in the first spectral line pair, and the higher order spectral lines are negligible.

The sinusoidal vibration-induced spectral lines $\mathcal{L}'(f_v)$ in the phase noise can be calculated from Equation (B.11). For example, if $|\vec{\Gamma}| = 1 \times 10^{-9}/g$ and $f_o = 10$ MHz, then even if the oscillator is completely noise-free at rest, the spectral lines in the phase noise spectrum, $\mathcal{L}'(f_v)$, at a sinusoidal vibration level of 1g along $\vec{\Gamma}$ will be as shown in Table B.1.

C. Random Vibration Example

For a small modulation index, random vibration's contribution to phase noise is given by:

$$\mathcal{L}(f) = 20 \log \left(\frac{\vec{\Gamma} \cdot \vec{A} f_o}{2f} \right), \tag{B.12}$$

where $|\vec{A}| = [2(PSD)]^{1/2}$ and PSD is the power spectral density of the vibration. The use of $\mathcal{L}(f)$ is in conformance with IEEE-1139-1988 [11]. As can be seen from the following examples, vibrating platforms can cause severe phase noise degradations.

Table B.1
Spectral Lines due to Sinusoidal Vibration ($|\vec{\Gamma}| = 1 \times 10^{-9}$/g, f_o = 10MHz, $|\vec{A}|$ = 1g)

f_v, in Hz	$\mathcal{L}'(f_v)$, in dBc
1	-46
10	-66
100	-86
1,000	-106
10,000	-126

Random vibration-induced phase noise can be calculated from Equation (B.12). For example, if $|\vec{\Gamma}| = 1 \times 10^{-9}$/g and f_o = 10 MHz, then even if the oscillator is completely noise free at rest, the phase noise due solely to a vibration PSD of 0.1g^2/Hz along $\vec{\Gamma}$ will be as shown in Table B.2.

Table B.2
Sidebands due to Random Vibration ($|\vec{\Gamma}| = 1 \times 10^{-9}$/g, f_o = 10MHz, PSD = 0.1g^2/Hz)

Offset freq., f, in Hz	$\mathcal{L}(f)$, in dBc/Hz
1	-53
10	-73
100	-93
1,000	-113
10,000	-133

Figure B.1 shows a typical aircraft random vibration specification (power spectral density vs. vibration frequency is shown in the upper right portion of the figure) and the resulting vibration-induced phase noise degradation.

D. Large Modulation Index

The sideband levels at large modulation indices can be calculated from Equation (B.10). For example, at 5g acceleration, the vibration-induced spectral lines in the phase noise spectrum produced by a 1575 MHz oscillator, or a 5 MHz oscillator multiplied by 315, both with $|\vec{\Gamma}| = 2 \times 10^{-9}$/g, are shown in Table B.3. It can be seen that at f_v= 5.25 Hz, the sidebands are larger than the carrier.

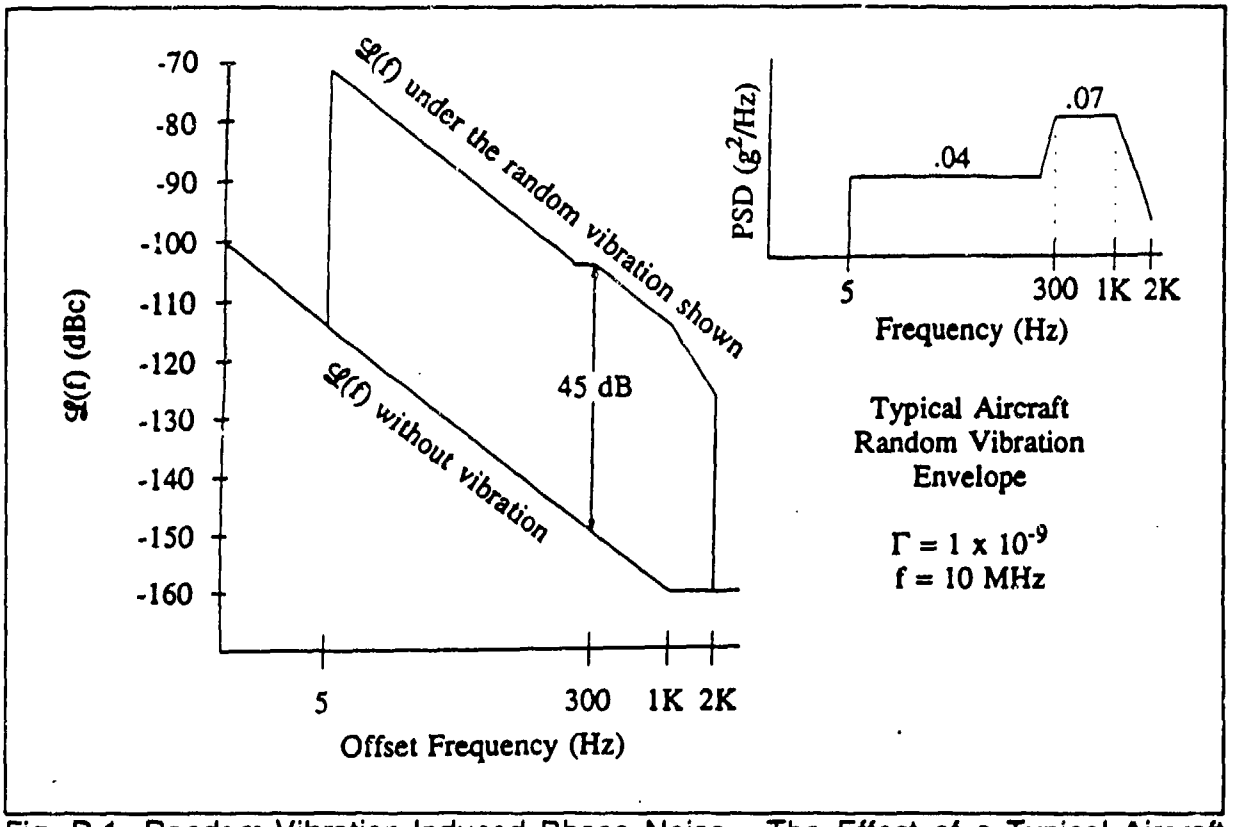

Fig. B.1. Random-Vibration-Induced Phase Noise - The Effect of a Typical Aircraft Random Vibration Envelope.

In a Rb frequency standard (as well as in other atomic frequency standards), the "carrier collapse" effect can cause a loss of microwave excitation power [3,4]. Modest acceleration levels can produce such a problem at low vibration frequencies. For example, when f_v = 10 Hz and $|\vec{\Gamma}| = 2 \times 10^{-9}$ per g, the peak acceleration level along $\vec{\Gamma}$ which produces $\beta = 2.4$ (since $J_0(2.4) = 0$) is

$$|\vec{a}| = \frac{(2.4)(10)}{(2 \times 10^{-9})(6.834 \times 10^9)} = 1.8g. \tag{B.13}$$

E. Integrated Phase Noise and Phase Excursion

The integrated phase noise for the bandwidth f_1 to f_2 is

$$\Delta\phi_i^2 = \int_{f_1}^{f_2} S_\phi(f)\,df. \tag{B.14}$$

For random vibration, it can be shown that

$$S_\phi(f) = \frac{1}{2f_v^2}(PSD)(|\vec{\Gamma}|\,f_o)^2. \tag{B.15}$$

Table B.3
Large Modulation Index Example ($|\vec{\Gamma}| = 2 \times 10^{-9}$/g, f_o = 1575 MHz, $|\vec{A}|$ = 5g)

f_v(Hz)	β	$\mathcal{L}'(f_v)$(dBc)
5.25	3.15	+2.3
25	0.63	-9.6
50	0.315	-16.0
500	0.0315	-36.0

When the oscillator is subjected to a simple sinusoidal vibration, the peak phase excursion follows from Equation (B.6), i.e.,

$$\Delta \phi_{peak} = \Delta f / f_v \ . \tag{B.16}$$

One can use the example in Figure B.1 to illustrate the effects of vibration on integrated phase noise. The power spectral density of the vibration, in g^2/Hz, is 0.04 from 5 Hz to 220 Hz, $0.07(f_v/300)^2$ from 220 Hz to 300 Hz, 0.07 from 300 Hz to 1000 Hz, and $0.07(f_v/1000)^{-2}$ from 1000 Hz to 2000 Hz. In the frequency band of 1 Hz to 2 kHz, the phase instability of the nonvibrating oscillator is

$$\begin{aligned} S_\phi(f) &= 2 \times 10^{-10}/f^2 \quad f \le 1\ KHz \\ S_\phi(f) &= 2 \times 10^{-16} \quad\quad f \ge 1\ KHz \end{aligned} \tag{B.17}$$

and, from Equation (B.14), the integrated phase noise from 1 Hz to 2 kHz is

$$\phi_i^2 \sim 2 \times 10^{-10}\ radians^2 \ . \tag{B.18}$$

Therefore,

$$\phi_i = 1.4 \times 10^{-5}\ radians \ . \tag{B.19}$$

While the oscillator is vibrating, the integrated phase noise is

$$\begin{aligned} \phi_i^2 = & \int_1^5 (2 \times 10^{-10}/f^2)\, df + \int_5^{220} (0.04)(0.01/f)^2 df \\ & + \int_{220}^{300} (0.07)(0.01/300)^2 df \\ & + \int_{300}^{1000} (0.07)(0.01/f)^2 df + \int_{1000}^{2000} (0.07)(0.01 * 1000)^2/f^4\, df \\ = & \ 8 \times 10^{-7}\ radians^2 \ . \end{aligned} \tag{B.20}$$

Therefore,

$$\phi_i = 9 \times 10^{-4}\ radians \ . \tag{B.21}$$

It can be seen that the integrated phase noise ϕ_i^2 during vibration is 4000 times that of the noise when the oscillator is not vibrating, and the rms phase deviation, ϕ_i, is about 60 times larger during vibration. When the frequency is multiplied from 10 MHz to 10 GHz; e.g., as it might be in a radar system, the rms phase deviation increases to 0.9 radian, which can be catastrophic to systems.

Appendix C - Analysis of 2-g Tipover Test Results

The effect of a gravitational field on an oscillator is a body force acting upon the internal components. Acceleration is defined as the second derivative of displacement with time. The effect of a gravitational field is opposite in sense to an acceleration effect. Figure C.1 shows this relationship between a gravitational field and acceleration. One way to handle this effect is to use $\vec{a} = -\vec{g}$.

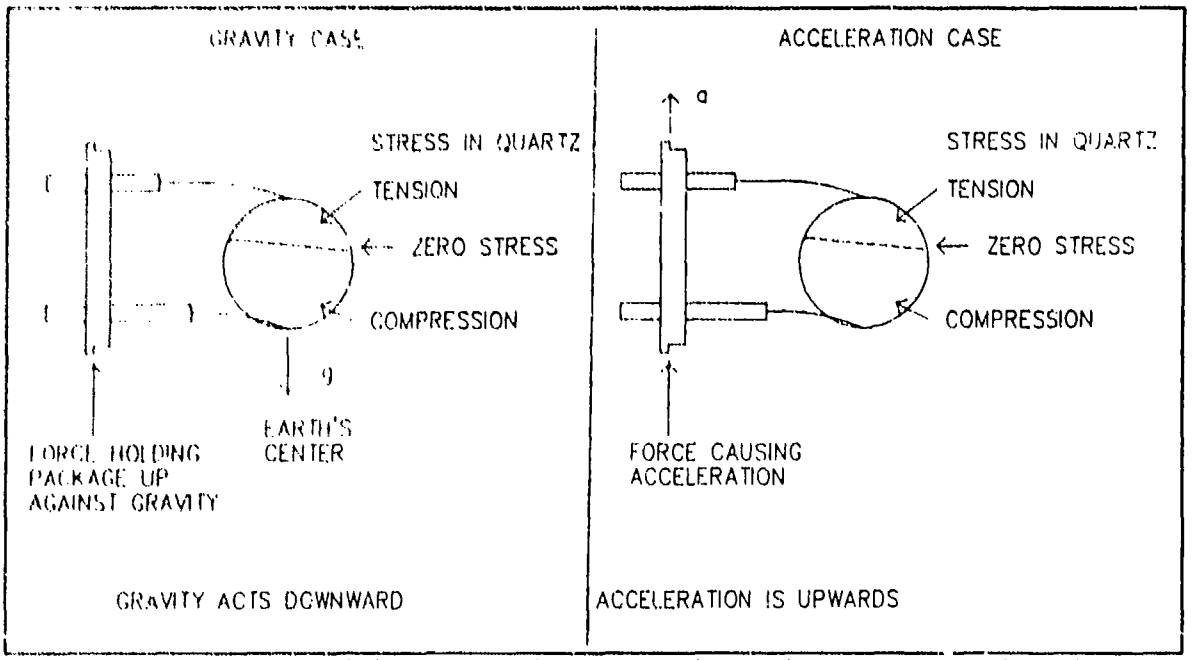

Fig. C.1. Comparison of Gravitational Effect and Acceleration Effect Showing that Opposite Direction Definition Causes the Same Stress Pattern in the Quartz and, thus, the Same Frequency Shift.

Referring to Figure C.2, let $\hat{x}$, $\hat{y}$ and $\hat{z}$ be the unit vectors fixed to the major axes X, Y, and Z of the oscillator; $\hat{i}$, $\hat{j}$ and $\hat{k}$ be the unit vectors fixed to the test bench; and $\vec{g}$ be gravity, of magnitude g and direction $-\hat{j}$. Also, let γ_x, γ_y and γ_z be the components of $\vec{\Gamma}$ along $\hat{x}$, $\hat{y}$ and $\hat{z}$ so that

$$\vec{\Gamma} = \gamma_x \hat{x} + \gamma_y \hat{y} + \gamma_z \hat{z} \tag{C.1}$$

In the 2-g tipover test, $f(\vec{a}) = f(\vec{g})$, which can be expressed as (using $\vec{a} = -\vec{g}$)

$$f(\vec{g}) = f_o(1 - \vec{\Gamma} \cdot \vec{g}) = f_o[1 + g\gamma_x(\hat{j}\cdot\hat{x}) + g\gamma_y(\hat{j}\cdot\hat{y}) + g\gamma_z(\hat{j}\cdot\hat{z})] \tag{C.2}$$

If, initially, $\hat{x}$, $\hat{y}$ and $\hat{z}$ are parallel to $\hat{i}$, $\hat{j}$ and $\hat{k}$, and if we start the test by rotating the oscillator counterclockwise about the $\hat{z}$ (or $\hat{k}$) axis, and if we define the angle between $\hat{i}$ and $\hat{x}$ as θ, then in Equation (B.2)

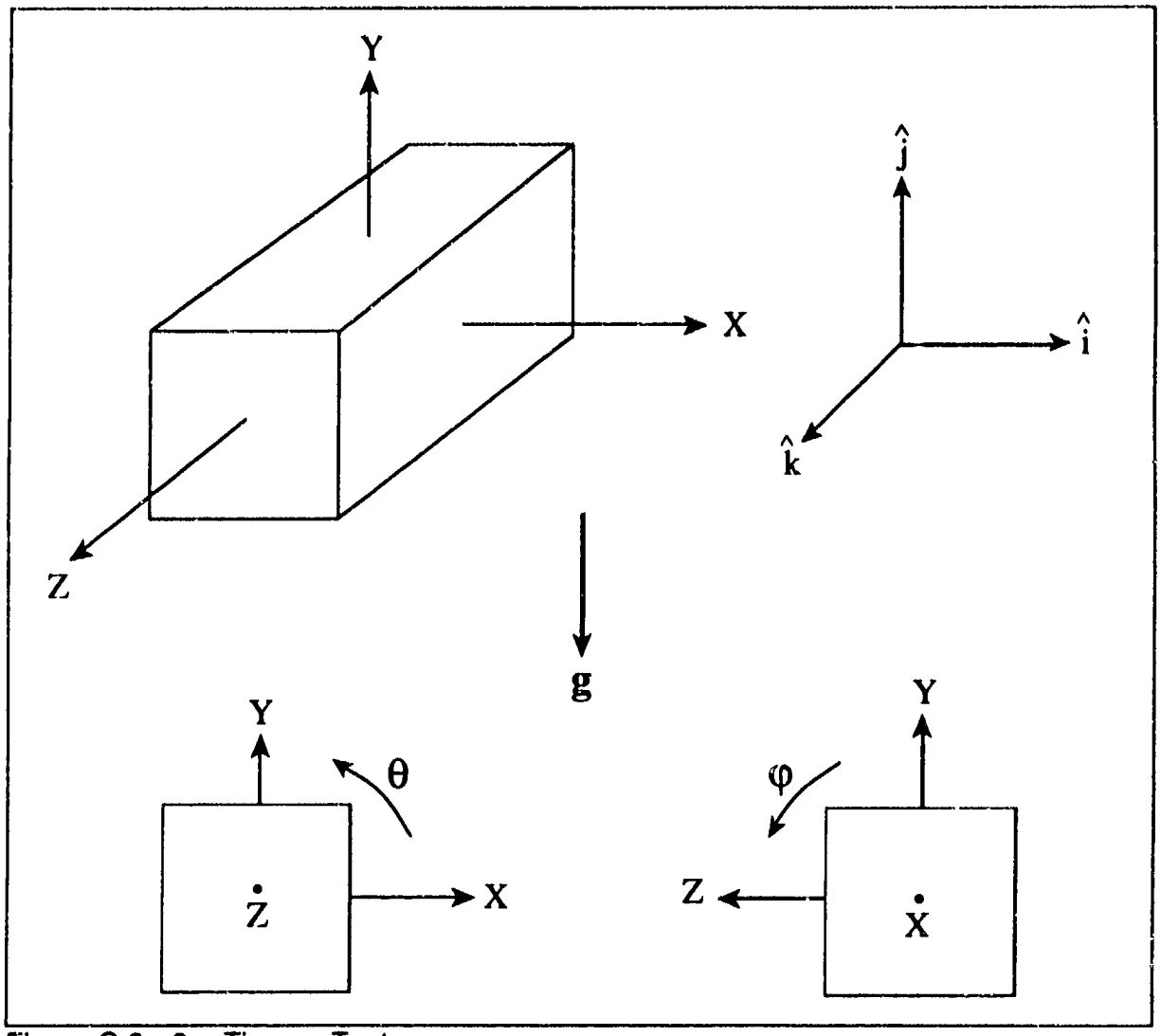

Figure C.2. 2-g Tipover Test

$$\hat{j} \cdot \hat{x} = \cos(90° - \theta) = \sin\theta \tag{C.3}$$

$$\hat{j} \cdot \hat{y} = \cos\theta \tag{C.4}$$

$$\hat{j} \cdot \hat{z} = \cos(90°) = 0 \tag{C.5}$$

and $f(\vec{g})$ becomes a function of θ, where

$$f(\theta) = f_o(1 + g\gamma_x \sin\theta + g\gamma_y \cos\theta). \tag{C.6}$$

The normalized frequency change during rotation, per g, is

$$\frac{\Delta f(\theta)}{f_o g} = \frac{f(\theta) - f(0)}{f_o g} = (1 + \gamma_x \sin\theta + \gamma_y \cos\theta) - (1 + \gamma_y) \qquad (C.7)$$
$$= \gamma_x \sin\theta + \gamma_y (\cos\theta - 1)$$

which can be written as

$$\frac{\Delta f(\theta)}{f_o g} = M \sin(\theta + D) - M \sin D \qquad (C.8)$$

where

$$M^2 = \gamma_x^2 + \gamma_y^2; \quad D = \tan^{-1}\left(\frac{\gamma_y}{\gamma_x}\right); \quad \gamma_x = M \cos D; \quad \gamma_y = M \sin D. \qquad (C.9)$$

Equation (C.8) shows that $\Delta f(\theta)$ vs. θ is a sinusoidal function.

From a least-squares fit to the $\Delta f(\theta)$ vs. θ data (e.g., to the 16 data points while rotating 360° in 22.5° steps about one axis, as shown in Figure 1), we can determine γ_x and γ_y. To determine γ_z, let us rotate the oscillator about the $\hat{x}$ axis, starting with $\hat{x}$ parallel to $\hat{k}$, $\hat{y}$ parallel to $\hat{j}$, and $\hat{z}$ parallel to $-\hat{i}$. If ϕ is the angle between $-\hat{z}$ and $\hat{i}$, then

$$\hat{j} \cdot \hat{x} = 0 \qquad (C.10)$$

$$\hat{j} \cdot \hat{y} = \cos\phi \qquad (C.11)$$

$$\hat{j} \cdot \hat{z} = \cos(\phi + 90°) \qquad (C.12)$$

and

$$\frac{\Delta f(\phi)}{f_o g} = \gamma_y (\cos\phi - 1) - \gamma_z \sin\phi. \qquad (C.13)$$

From a least-squares fit to the $\Delta f(\phi)$ vs. ϕ data, we can determine γ_z, and obtain a self-consistency check on γ_y. Similarly, from a rotation about the y-axis, we can obtain a self-consistency check for γ_x and γ_z.

Appendix D - Acceleration Effects in Crystal Filters

A. General

Crystal filters are used in frequency sources to improve the output spectrum by attenuating far-out amplitude and phase noise as well as harmonics and other spurious outputs. In this application, they are often called spectrum cleanup filters; however, it is well-known that under vibration such filters modulate the signals passing through them, adding as well as removing vibration-related sidebands. That is, the filter adds its own vibration-induced sidebands to those of the signals it passes. Accordingly, the use of a cleanup filter, or post-filter, is not the solution to every phase-noise problem [18]. In this section, we explore these effects in greater detail.

In a properly designed and constructed crystal filter, the crystal resonators are the principal vibration-sensitive components. To ensure that this is so, care must be given to the selection of other components, particularly inductors, transformers, and variable capacitors, and to mechanical design. These considerations are not trivial, but detailed discussion is beyond the scope of this document, which will consider only crystal-related effects.

Consider a frequency source whose nominally sinusoidal output is frequency-modulated due to vibration and then passed through a filter which is also subject to vibration. (The two vibration environments will be assumed to be the same, although this is not necessarily the case; e.g., if either the source or the filter is protected by vibration isolators.) The filter, in turn, modulates both the carrier and the vibration sidebands of the source; however, modulation of the latter, being a second-order effect, can ordinarily be neglected. Hence, the vibration sidebands of the filter output are essentially the vector sum of the sidebands of the source, attenuated and phase-shifted by the filter, and the sidebands due to the modulation of the carrier by the filter.

Analytically, a filter under vibration is a time-varying linear system. At vibration frequencies which are much less than one-half the filter passband width, the modulation due to vibration of the filter can be estimated from a quasi-static analysis. In the quasi-static case, if all of the resonators have identical $\vec{\Gamma}$'s, acceleration produces a shift of the filter center frequency equal to the frequency shift of the resonators, $\Delta f = \vec{\Gamma} \cdot \vec{A} \cdot f_o$. This modulates the phase of the carrier by $2\pi\Delta f \cdot Tg(f_c)$, where $Tg(f_c)$ is the filter group delay at the carrier frequency. When the resonators have different $\vec{\Gamma}$'s, a quasi-static analysis can still be performed by considering the sensitivity of the filter phase characteristic to each resonator frequency.

While the quasi-static viewpoint is useful for some signal-processing applications, in spectrum cleanup applications very narrow filters are often used for which the quasi-static analysis is inadequate. In the next section, an expression for the vibration-induced sidebands in a one-pole filter, valid for all vibration frequencies, is given; then the source's

sidebands are added in to obtain the net effect of the filter. Section C then presents normalized results for a two-pole Butterworth post-filter.

B. Single-Resonator Filter

The inadequacy of the quasi-static point of view was shown for a single-resonator (one-pole) filter by Horton and Morley [28] who observed that for sinusoidal vibration at frequency f_v and a sinusoidal input at a carrier frequency, f_o, the output is a phase-modulated signal[3] for which, for small phase deviation,

$$\mathcal{L}'(f_v) = 20 \log(\vec{\Gamma} \cdot \vec{A} \cdot Q_L / [1 + (2 Q_L f_v / f_o)^2]^{1/2}) . \quad (D.1)$$

Since the 3 dB bandwidth of a one-pole filter is

$$BW = f_o / Q_L , \quad (D.2)$$

where Q_L is the loaded Q, Equation (D.1) can be written

$$\mathcal{L}'(f_v) = 20 \log(\vec{\Gamma} \cdot \vec{A} \cdot (f_o / BW) / [1 + (f_v / BW/2)^2]^{1/2}) . \quad (D.3)$$

From Equations (D.1) and (D.3) it can be seen that the phase modulation exhibits a frequency dependence corresponding to a one-pole filter gain characteristic. For vibration frequencies within the filter passband, the denominator in Equation (D.3) is approximately 1 and the vibration-induced phase noise is nearly constant at the level predicted by quasi-static analysis. On the other hand, for vibration frequencies far removed from the passband, Equation (D.1) is asymptotic to Equation (B.11). Thus, at low vibration frequencies the filter's contribution to vibration-induced phase noise is less than that of a crystal oscillator using the same resonator (or, in general, any frequency source having the same acceleration sensitivity) while at high vibration frequencies the two contributions are the same. This is illustrated in Figure D.1. The curve labelled "filter" represents the phase modulation of a sinusoidal carrier by the filter; "oscillator," the phase modulation present on the unfiltered oscillator output; and "filter + oscillator" the phase modulation at the filter output, discussed below. The vibration frequency is normalized to one-half the 3 dB bandwidth, BW, of the filter; the sideband levels are shown relative to the unfiltered oscillator sideband level at BW/2.

The curve labelled "Filter + Oscillator" represents the vector sum of the sidebands of the source, attenuated and phase-shifted by the filter, and the sidebands added by the

[3] There is, of course, some amplitude modulation as well. Because the amplitude response of the filter is an even function of frequency, while the phase response is odd, the amount of AM is generally negligible. Further, if the filter center frequency and the carrier frequency are the same, then the AM sidebands occur only at $2f_v$, $4f_v$, etc.

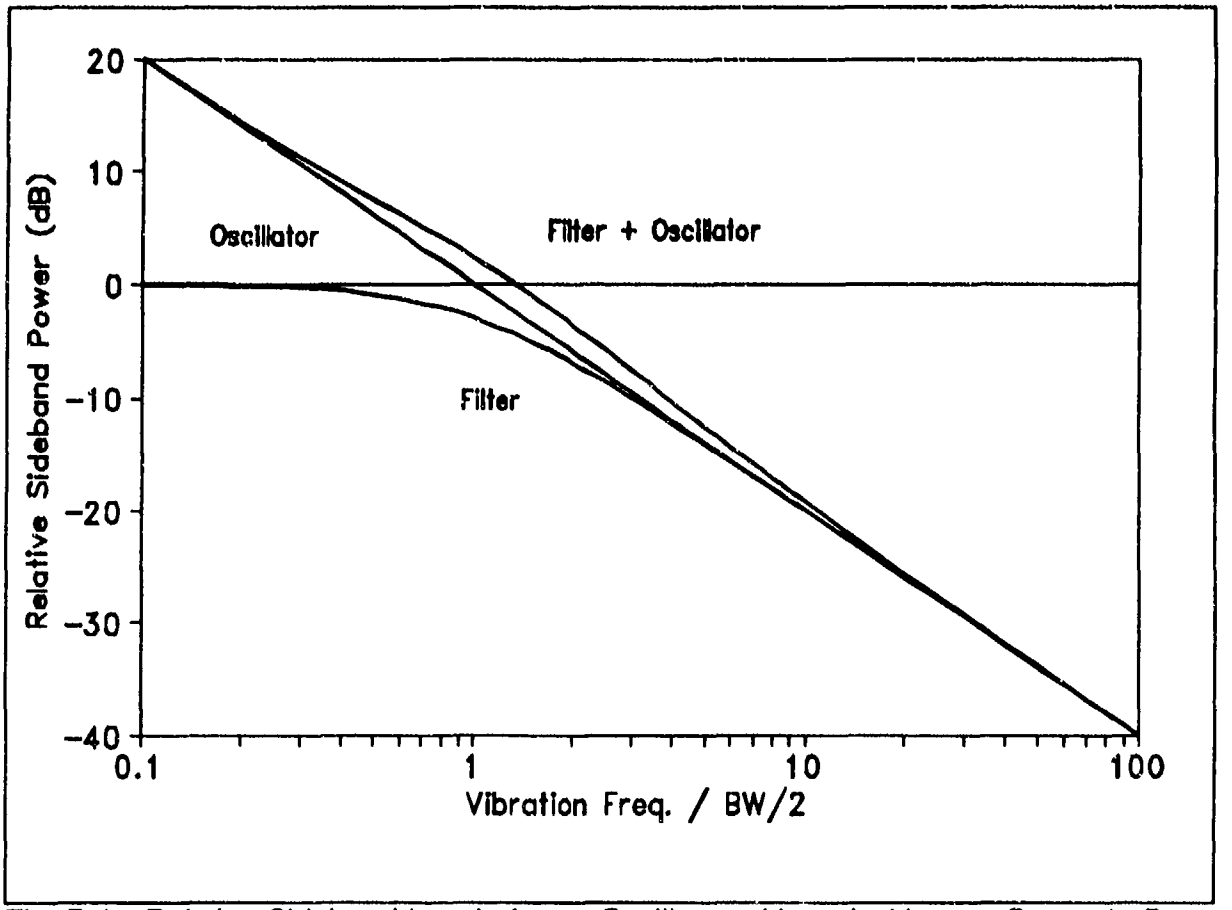

Fig. D.1. Relative Sideband Levels for an Oscillator with and without a One-pole Post-Filter when the Filter Resonator has the Same Acceleration Sensitivity as the Oscillator.

filter.[4] It can be seen that for identical gamma vectors identically oriented, the single-pole filter does not improve the output phase modulation, but rather degrades it by as much as 2.5 dB in the vicinity of the passband edges. (However, if the gamma vectors of the source and filter were oriented anti-parallel instead of parallel, some improvement would occur in the same region.) For vibration frequencies much greater than or much less than BW/2, the vibration-induced sideband level is essentially unchanged by the filter. This means that the filter may still play a useful role in cleaning up spurious responses, etc., but in order to reduce the vibration-related sidebands the filter resonator's acceleration sensitivity must be less than the frequency source's.

An example is given in Figure D.2 for a 10 MHz oscillator having a g-sensitivity of 5×10^{-10}/g with a single-pole post-filter whose resonator has the same g-sensitivity as the

[4] There is a further $\pi/2$ phase shift between the sidebands of the frequency source, which arise from a frequency modulation process, and the sidebands due to the filter, which are produced by phase modulation.

oscillator. For this example, the acceleration is taken as 1 g in the direction of the gamma vector. The filter 3 dB bandwidth is 100 Hz (BW/2 = 50 Hz), corresponding to a loaded Q of 1×10^6.

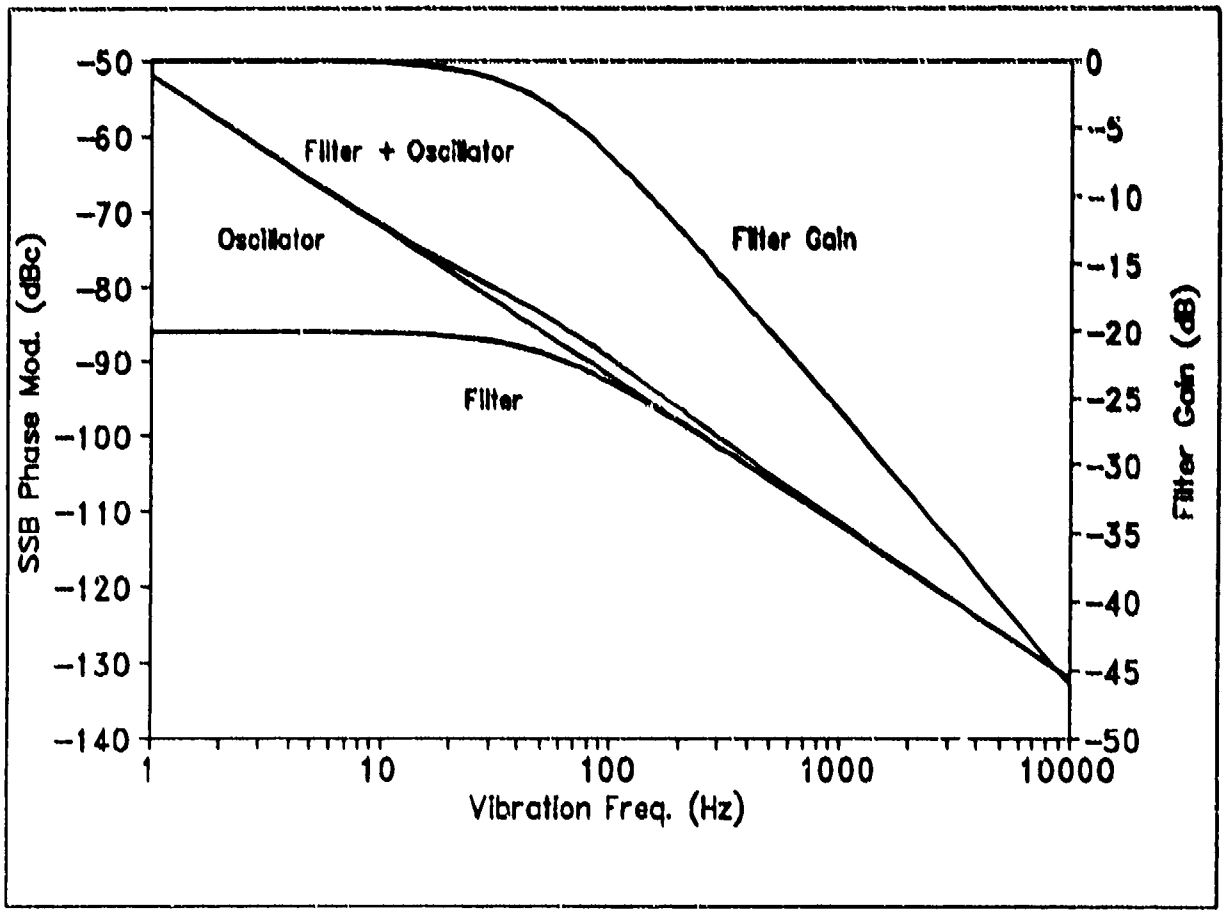

Fig. D.2. Sideband Levels for a 10 MHz Oscillator, $|\vec{\Gamma}| = 5 \times 10^{-10}/g$, with and without a One-pole Post-filter (BW/2 = 50 Hz) Whose Resonator has the same Acceleration Sensitivity as the Oscillator.

To help understand the trade-offs, consider two vibration frequencies. At $f_v = 50$ Hz, $\mathcal{L}'_v$ is -86 dBc for the oscillator alone, -89 dBc for the filter alone, and -83.7 dBc for the filtered output. If the filter's g-sensitivity were small enough to be neglected (or if it is provided with vibration isolation), then the filtered output would be -89 dBc, since the filter provides 3 dB of attenuation. Similarly, at $f_v = 500$ Hz, $\mathcal{L}'_v$ is -106 dBc for the oscillator alone, -106 dBc for the filter alone, and -105.2 dBc for the filtered output. If, again, the filter's g-sensitivity were small enough to be neglected, then the filtered output would be -126 dBc, corresponding to the 20 dB of attenuation provided by the filter.

C. Multiresonator Filters

For the one-pole filter, the vibration-induced phase modulation turned out to be attenuated by the filter gain. For filters of higher order, things are not so simple, even for filters having identical resonators. Since the resonators, each of which is modulating the signal, are distributed throughout the filter network, their respective contributions to the filter's acceleration sensitivity are not the same. At low vibration frequencies, quasi-static analysis is valid; otherwise, a detailed analysis must be performed [18,28].

In general, the vibration-induced resonator frequency changes may differ in magnitude and sign, so that the net effect is to produce both amplitude and phase modulation, although ordinarily, for signals in the passband of the filter, the principal effect is phase modulation. (Further, if the filter assembly is not adequately rigid, the vibration-induced motion of the several resonators may differ in magnitude and phase, in which case analysis is not likely to be practical, since it must take account of structural effects.)

Figure D.3 shows the sideband levels for a two-pole Butterworth filter when the acceleration sensitivities of the two filter resonators are the same in magnitude and orientation as that of the oscillator, and the center frequency of the filter equals the oscillator frequency. It is seen that the filter provides no net improvement in the vibration-induced sidebands and a degradation of 3 dB at the filter passband edge.

The net effect of the filter is more easily seen in Figure D.4, which shows the vibration sideband reduction for the two-pole Butterworth as a function of normalized vibration frequency, with the gamma ratio, defined as $|\vec{\Gamma}_{\text{filter crystal}}|/|\vec{\Gamma}_{\text{source}}|$, as a parameter. Three curves are shown. A gamma ratio of 1 corresponds to the equal-gamma case Figure D.3; a ratio of 0.5, to the case in which the acceleration sensitivity of the filter crystals is one-half that of the source; and a ratio of 0.2 to the case in which the acceleration sensitivity of the filter crystals is one-fifth that of the source.

The relative contributions of the filter resonators can only be touched upon here, since a given filter characteristic can be realized by many different circuit configurations. If our two-pole example is realized as a ladder network or as two one-pole half-lattice sections in tandem, then, at low vibration frequencies, both resonators contribute equally, while at frequencies in the stopband the resonator nearer the output port is the primary contributor to vibration-induced modulation. Additionally, the relative contributions of the resonators may be expected to change as a function of the frequency of the source relative to the filter center frequency, so that any cancellation technique will be limited to a narrow range of vibration frequencies.

D. Conclusions About the Use of Crystal Filters for Spectrum Cleanup

While spectrum cleanup filters play a valuable role in the reduction of spurious outputs in frequency sources, they do not solve the problem of acceleration sensitivity. The examples given here are representative: in order for a post-filter to reduce the

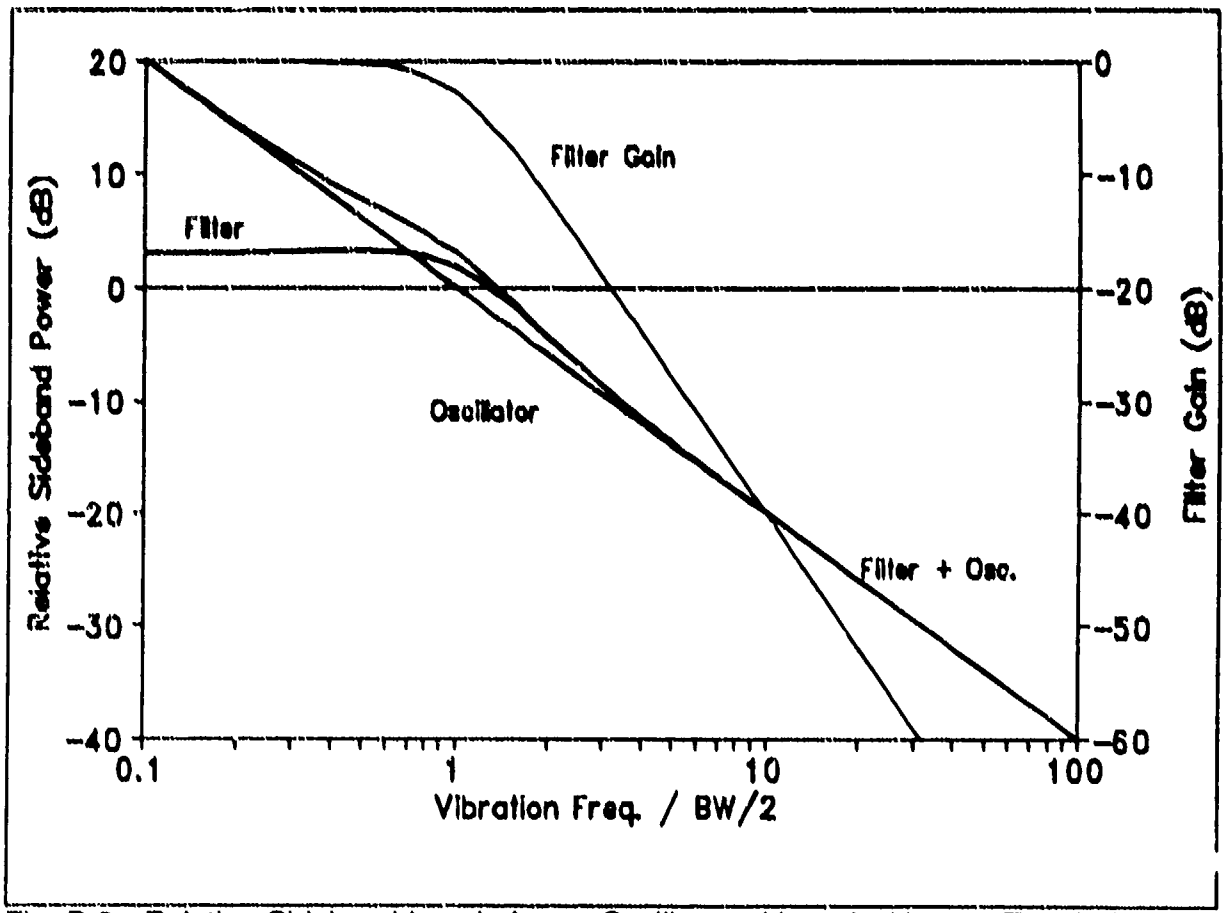

Fig. D.3. Relative Sideband Levels for an Oscillator with and without a Two-Pole Post-filter when the Filter Resonators have the Same Acceleration Sensitivity as the Oscillator.

vibration-induced sidebands of a frequency source, it must have either mechanical isolation or resonators whose g-sensitivity is better than that of the frequency source. Although the treatment has been in terms of sinusoidal vibration, the extension to other vibration spectra is obvious.

Acceleration effects in crystal filters are also of importance in a variety of signal-processing applications which are beyond the scope of this document. The considerations for these are somewhat different than for spectrum cleanup, although the basic relations are the same.

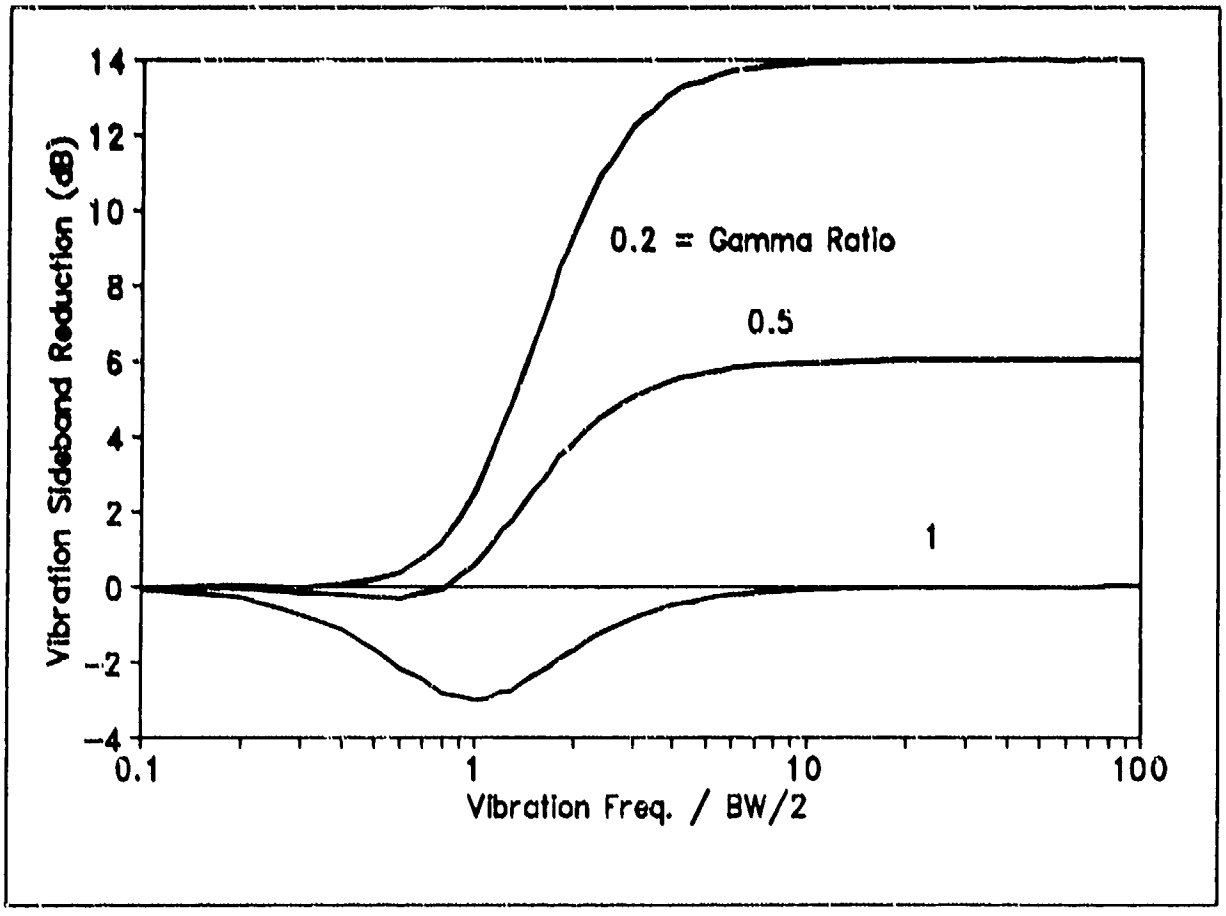

Fig. D.4. Reduction in Vibration Sideband Levels for a Source with a Two-pole Butterworth Post-filter, for Three Values of the Gamma Ratio, $|\vec{\Gamma}_{\text{filter crystal}}|/|\vec{\Gamma}_{\text{source}}|$.

Appendix E

Acceleration-Relevant Paragraphs from MIL-O-55310C[5]

A. Requirements

3.1 Specification sheets. The individual item requirements shall be as specified herein in and in accordance with the applicable specification sheet. In the event of any conflict between the requirements of this specification and the specification sheet, the latter shall govern.

3.7.16 Short-term stability (see 6.3.26 and 6.3.29) (when specified, see 3.1).

3.7.16.2 Phase noise, random vibration (when specified, see 3.1). When measured as specified in 4.9.17.2, the phase noise, $\mathcal{L}(f)$ (see 6.3.28), shall not exceed the values specified for the random vibration levels and spectra specified.

3.7.16.3 Phase noise, acoustic (when specified, see 3.1). When measured as specified in 4.9.17.3, the phase noise, $\mathcal{L}(f)$ (see 6.3.28), shall not exceed the values specified for the acoustic intensities and spectra specified.

3.7.17 Acceleration sensitivity (see 6.3.30) (when specified, see 3.1).

3.7.17.1 Acceleration sensitivity, steady-state (when specified, see 3.1). When tested as specified in 4.9.18.1, the frequency change per unit of acceleration shall not exceed the value specified at acceleration levels up to the maximum specified.

3.7.17.2 Acceleration sensitivity, 2g tip-over (when specified, see 3.1). When tested as specified in 4.9.18.2, the acceleration sensitivity due to 2g tip-over shall not exceed the value specified. If specified, the maximum acceleration sensitivity shall be in the direction specified. If specified, the direction of the acceleration sensitivity vector (expressed in terms of its three unit vectors) shall be recorded and supplied with serial number for each oscillator produced.

3.7.17.3 Acceleration sensitivity, vibration (when specified, see 3.1). When tested as specified in 4.9.18.3, the low level acceleration sensitivity shall not exceed the value specified for the maximum acceleration specified. If specified, the maximum acceleration sensitivity shall be in the direction specified. If specified, the direction of the acceleration sensitivity vector (expressed in terms

---

[5] In MIL-O-55310, section 3 (paragraphs 3.1 to 3.9.2.6) contains the "Requirements." and section 4, the corresponding "Quality Assurance Provisions." Section 6 contains definitions.

of its three unit vectors) shall be recorded and supplied with serial number for each oscillator produced.

3.7.31 Accumulated time error (when specified, see 3.2). When tested in accordance with 4.9.32, the time integral of fractional frequency change for a specified time interval resulting from specified time variant conditions (temperature, acceleration, radiation, etc.) shall not exceed the values specified.

3.7.32 Clock accuracy (type 7) (see 6.3.40).

3.7.32.1 Clock accuracy (corrected pulse train output). When tested in accordance with 4.9.33.1, the clock accuracy of a microcomputer compensated crystal oscillator with a time-corrected pulse train output, operating over the specified conditions (temperature, acceleration, radiation, etc.) for the specified duration after syntonization and synchronization, shall not exceed the value specified (see 3.2).

3.7.32.2 Clock accuracy (digital time-of-day output). When tested in accordance with 4.9.33.2, the clock accuracy of a microcomputer compensated crystal oscillator with a digital clock time-of-day output, operating over the specified conditions (temperature, acceleration, radiation, etc.) for the specified duration after syntonization and synchronization, shall not exceed the value specified (see 3.2).

3.7.37 Vibration.

3.7.37.1 Vibration, sinusoidal (nonoperating). After undergoing the test specified in 4.9.38.1, the oscillator shall be capable of operation. Unless otherwise specified (see 3.1), the requirements specified in 3.7.4, 3.7.19, and 3.7.36 shall be met.

3.7.37.2 Vibration, sinusoidal (operating) (when specified, see 3.1). While undergoing the test as specified in 4.9.38.2, the oscillator shall be capable of operation. Unless otherwise specified (see 3.1), during the test, the requirements specified in 3.7.4 and 3.7.19 shall be met. The requirements in 3.7.17.3 shall be met when specified.

Unless otherwise specified (see 3.1), following the above tests, the requirements of 3.7.36 shall be met.

3.7.37.3 Vibration, random (nonoperating) (when specified, see 3.1). After undergoing the test specified in 4.9.38.3, the oscillator shall be capable of operation. Unless otherwise specified (see 3.1), the requirements specified in 3.7.4, 3.7.19, and 3.7.36 shall be met.

3.7.37.4 Vibration, random (operating) (when specified, see 3.1). While undergoing the test as specified in 4.9.38.4, the oscillator shall be capable of operation. Unless otherwise specified (see 3.1), during the test, the requirements specified in 3.7.4 and 3.7.19 shall be met. The requirements in 3.7.16.2 shall be met when specified.

Unless otherwise specified (see 3.1), following the above tests, the requirements of 3.7.36 shall be met.

3.7.38 Acoustic noise (operating) (when specified, see 3.1). While undergoing the test as specified in 4.9.39, the oscillator shall be capable of operation. Unless otherwise specified (see 3.1) during the test, the requirements specified in 3.7.4 and 3.7.19 shall be met. The requirements in 3.7.16.3 shall be met when specified.

Unless otherwise specified (see 3.1), following the above tests, the requirements of 3.7.36 shall be met.

3.7.39 Shock (specified pulse) (nonoperating). After undergoing the test specified in 4.9.40, the oscillator shall be capable of operation. Unless otherwise specified (see 3.1) the requirements specified in 3.7.1, 3.7.4, 3.7.9 (frequency-adjustable oscillators only), 3.7.13, 3.7.19, and 3.7.36 shall be met. The requirements of 3.7.10 shall be met when specified.

3.7.40 Acceleration (when specified, see 3.1).

3.7.40.1 Acceleration (nonoperating) (when specified, see 3.1). After undergoing the test specified in 4.9.41.1, the oscillator shall be capable of operation. Unless otherwise specified (see 3.1), the requirements specified in 3.7.1, 3.7.4, 3.7.19, and 3.7.36 shall be met.

3.7.40.2 Acceleration (operating) (when specified, see 3.1). While undergoing the test as specified in 4.9.41.2, the oscillator shall be capable of operation at all acceleration levels to the maximum specified. Unless otherwise specified, during the test, the requirements specified in 3.7.4, 3.7.17.1 and 3.7.19 shall be met.

Unless otherwise specified (see 3.1), following the above tests, the requirements specified in 3.7.36 shall be met.

3. Quality Assurance Provisions

4.9.17 Short-term stability (when specified, see 3.1) (see 3.7.16).

4.9.17.2 Phase noise, random vibration (when specified, see 3.1) (see 3.7.16.2

and 6.3.28). The oscillator shall be subjected to random vibration (operating) specified in 4.9.38.3. The spectral density of phase fluctuations, $S_\phi(f)$, shall be measured in accordance with NIST Technical Note 1337 and the test configuration of Figure 5 for the random vibration levels and spectra specified. The phase noise, expressed as $\mathcal{L}(f)$, in dBc per Hz, as defined in 6.3.28, shall not exceed the values specified.

4.9.17.3 Phase noise, acoustic (when specified, see 3.1) (see 3.7.16.3 and 6.3.28). The oscillators shall be subjected to "acoustic noise (operating)" specified in 4.9.39. The spectral density of phase fluctuations, $S_\phi(f)$, shall be measured in accordance with NIST Technical Note 1337 and the test configuration of Figure 5 for the acoustic noise intensities and spectra specified. The phase noise, expressed as $\mathcal{L}(f)$, in dBc per Hz, as defined in 6.3.28, shall not exceed the values specified.

4.9.18 Acceleration sensitivity (when specified, see 3.1) (see 3.7.17).

4.9.18.1 Acceleration sensitivity, steady-state (when specified, see 3.1) (see 3.7.17.1). The oscillator shall be subjected to "acceleration (operating)" specified in 4.9.41.2. Measurements shall be made at least 5 equally spaced acceleration levels between 20 percent of the maximum and the maximum specified. The frequency change per unit g of acceleration shall be determined graphically for all acceleration levels to the maximum specified. The following details shall apply:

a. Test configuration: See Figure 5.

b. Acceleration level: As specified (see 3.1).

c. Orientation (direction): As specified (see 3.1).

4.9.18.2 Acceleration sensitivity, 2g tip-over (when specified, see 3.1) (see 3.7.17.2). Three mutually perpendicular axes shall be defined relative to the external oscillator package. For each of the three axes, the following procedure shall be followed.

a. Position the oscillator with the ith axes vertical and the unit vector parallel to the positive ith axis pointing upward.

b. Record the frequency and call it f^+.

c. Position the oscillator with the ith axis vertical and the unit vector parallel to the negative ith axis pointing upward.

d. Record the frequency and call it f^-.

e. Calculate $\gamma_i = \dfrac{f_i^+ - f_i^-}{f_i^+ + f_i^-}$

After all three axes are measured, calculate the magnitude and direction of the acceleration sensitivity vector, Γ, as follows:

$$|\vec{\Gamma}| = \sqrt{\gamma_1^2 + \gamma_2^2 + \gamma_3^2}$$

and $$\vec{\Gamma} = \gamma_1\hat{i} + \gamma_2\hat{j} + \gamma_3\hat{k}$$

where i, j and k are the unit vectors parallel to the positive direction of axis 1, 2, and 3 respectively.

Precautions:

Care must be taken to ensure that the observed frequency changes are not due to gravitation-induced-thermal-convection-current changes within the oscillator. This condition is guarded against by performing the position change and frequency measurement as rapidly as possible. Verification is obtained by repeatable measured frequency changes following repetitive position changes inasmuch as the changes due to altered convection currents are generally not repeatable.

4.9.18.3 Acceleration sensitivity, vibration (when specified, see 3.1) (see 3.7.17.3).

4.9.18.3.1 Acceleration sensitivity, sinusoidal vibration. The oscillator shall be subjected to vibration, sinusoidal (operating) specified in 4.9.38.2. A sinusoidal excitation shall be applied to the vibration machine at a level not to exceed 20g's or the value specified. The frequency of vibration, f_v, shall be varied over the frequency range specified in a logarithmic progression of not fewer than 7 frequencies per decade. At each vibration frequency the relative sideband intensity, i.e., the ratio of the power in the upper vibration-induced sideband to the power at the unmodulated signal frequency, shall be determined. The acceleration sensitivity at each vibration frequency shall be determined from the following:

$$\gamma_i = \frac{2f_v\, 10^{(l_i(f_v)/20)}}{a_i\, v_o}$$

Where:

γ_i = Acceleration sensitivity along axis i (i=1, 2, or 3)

f_v = Vibration frequency
a_i = Acceleration frequency
v_o = Carrier frequency
$l_i(f_v)$ = Relative sideband intensity (power ratio) in dBc (see 6.3.28) when the vibration at frequency f_v is along the i axis.[6]

The acceleration sensitivity for each axis is the maximum value measured for any vibration in the range specified. The above procedure is repeated for two other axes such that the three axes are mutually perpendicular. The magnitude and direction of the acceleration sensitivity vector, $\vec{\Gamma}$, shall be calculated as specified in 4.9.18.2.

The following details apply:

a. Test configuration: See Figure 14.

b. Vibration level: As specified (see 3.1).

c. Vibration frequency range: As specified (see 3.1).

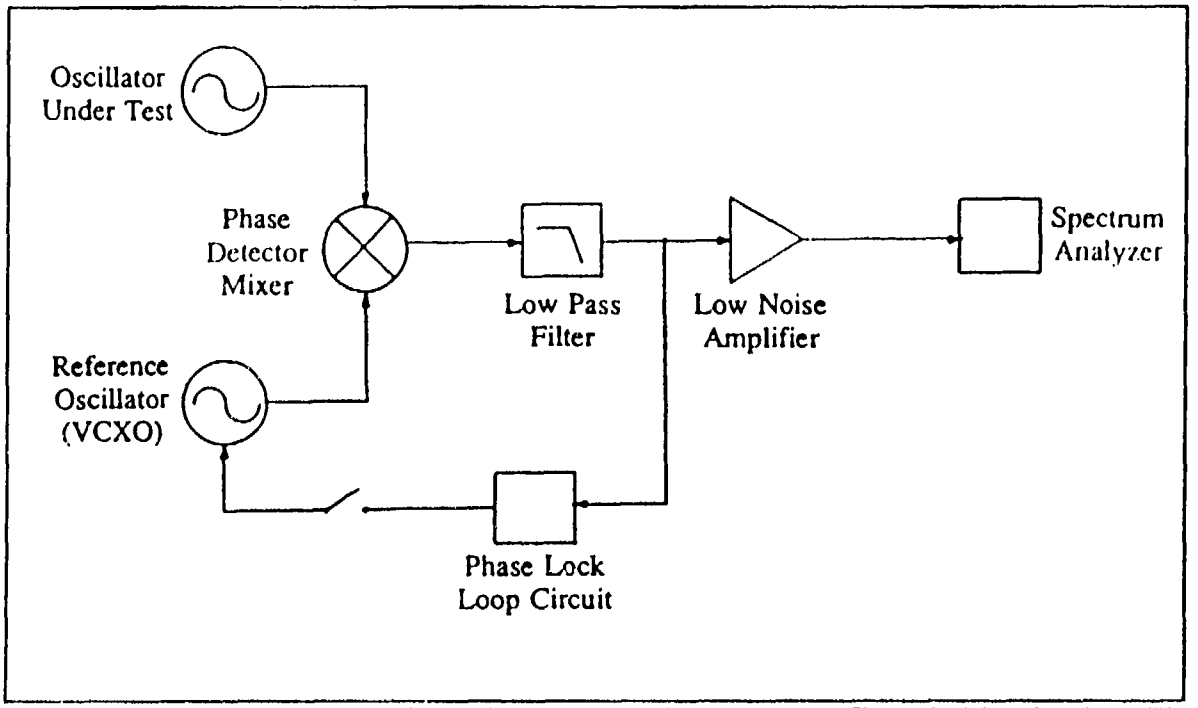

Fig. E.1. Quadrature Phase Detection Method (This figure is Fig. 5 in MIL-O-55310B).

4.9.18.3.2 Acceleration sensitivity, random vibration. It is acceptable to assume

[6]Note that $l_i(f_v)$ in MIL-0-55310C would be denoted by $L_i'(f_v)$ as in Eq. 2.9 on page 24.

that the acceleration sensitivity under random vibration is the same as under sinusoidal vibration. The sinusoidal vibration test method detailed in 4.9.18.3.1 is preferred for measuring the acceleration sensitivity of a crystal oscillator in a vibrating environment.

4.9.32 Accumulated time error (when specified, see 3.2) (see 3.7.31). The oscillator shall be subjected to the specified time variant conditions. The time integral of the induced frequency offset, for the specified time interval shall be determined.

4.9.33 Clock accuracy (see 3.7.32).

4.9.33.1 Clock accuracy (type 7) (corrected pulse train output) (see 3.7.32.1). The oscillator shall be subjected to the specified operating conditions (temperature, supply voltage, acceleration, radiation, etc.). The clock accuracy shall be determined by measurement of time error (or time errors, if effects are tested for separately) over the specified interval (or fraction thereof, if resulting frequency offset is constant) under the worst case combination of operating conditions.

4.9.33.2 Clock accuracy (type 7) (digital time-of-day output) (see 3.7.32.2). The clock accuracy shall be determined as specified in 4.9.33.1.

4.9.38 Vibration (see 3.7.37).

4.9.38.1 Vibration, sinusoidal (nonoperating) (see 3.7.37.1). The oscillator shall be tested in accordance with MIL-STD-202, method 204. The following details shall apply:

a. Method of mounting: Unless otherwise specified, see 3.1, the oscillator shall be attached by its normal mounting means to a rigid fixture capable of transmitting the specified vibration condition. There shall be no resonance in the mounting structure within the range of vibration frequencies specified.

b. Test condition letter: As specified (see 3.1).

c. Measurements: Unless otherwise specified (see 3.1).

(1) Before test: As specified in 4.9.37.

(2) After test: As specified in 4.9.5, 4.9.20, and 4.9.37.

4.9.38.2 Vibration, sinusoidal (operating) (when specified, see 3.1) (see 3.7.37.2). The energized oscillator shall be subjected to a sinusoidal vibration

test, as follows:

The oscillator shall be rigidly mounted to the platform of a vibration machine. A sinusoidal excitation shall be applied to the vibration machine at the level specified. The frequency of vibration shall be advanced over the frequency range specified in a logarithmic progression of no fewer than 7 frequencies per decade. At each vibration frequency the specified measurements shall be performed. The following details shall apply:

a. Mounting: As specified in 4.9.38.

b. Peak vibration level: As specified (see 3.1).

c. Frequency range: As specified (see 3.1).

d. Direction of motion: Three mutually perpendicular directions (unless otherwise specified, see 3.1).

e. Duration: 2 hours maximum (unless otherwise specified, see 3.1).

f. Measurements: Unless otherwise specified (see 3.1).

(1) Before test: As specified in 4.9.37.

(2) During test: As specified in 4.9.5, 4.9.18.3.1, and 4.9.20.

(3) After test: As specified in 4.9.37.

4.9.38.3 Vibration, random (nonoperating) (when specified, see 3.1) (see 3.7.37.3). The energized oscillators shall be tested in accordance with MIL-STD-202, method 204. The following details shall apply:

a. Mounting: As specified in 4.9.38.

b. Test condition: As specified (see 3.1).

c. Duration: As specified (see 3.1).

d. Measurements: Unless otherwise specified (see 3.1).

(1) Before test: As specified in 4.9.37.

(2) After test: As specified in 4.9.37.

4.9.38.4 Vibration, random (operating) (when specified, see 3.1) (see

3.7.37.4). The energized oscillator shall be subjected to a random vibration test, as follows:

The oscillator shall be rigidly mounted to the platform of a vibration machine. A random vibration shall be applied at the levels and frequencies of the vibration spectrum specified. The following details shall apply:

a. Mounting: As specified in 4.9.38.1.

b. Power-Spectral Density Curve: As specified (see 3.1).

c. Direction of Motion: Three mutually perpendicular directions (unless otherwise specified, see 3.1).

d. Duration: 15 minutes maximum on each axis (unless otherwise specified, see 3.1).

e. Measurements: Unless otherwise specified (see 3.1).

(1) Before test: As specified in 4.9.37.

(2) During test: As specified in 4.9.5, 4.9.17.2, and 4.9.20.

(3) After test: As specified in 4.9.37.

4.9.39 Acoustic noise (operating) (when specified, see 3.1) (see 3.7.38). The energized oscillator shall be tested in accordance with MIL-STD-810, method 515, procedure I. The following details shall apply:

a. Category: As specified (see 3.1).

b. Overall sound pressure: As specified (see 3.1).

c. Exposure time: As specified (see 3.1).

d. Measurements: Unless otherwise specified (see 3.1).

(1) Before test: As specified in 4.9.37.

(2) During test: As specified in 4.9.5, 4.9.17.3, and 4.9.20.

(3) After test: As specified in 4.9.37.

4.9.40 Shock (specified pulse) (nonoperating, see 3.7.39). The oscillator shall be tested in accordance with MIL-STD-202, method 213. The following details

shall apply:

a. Method of mounting: The oscillator shall be attached to a rigid fixture.

b. Test condition I (unless otherwise specified, see 3.1).

c. Number of blows: Two blows in each of the three mutually perpendicular axes.

d. Measurements: Unless otherwise specified (see 3.1).

(1) Before test: As specified in 4.9.37.

(2) After test: As specified in 4.9.2, 4.9.5, 4.9.10, 4.9.11, 4.9.14, 4.9.20, and 4.9.37.

4.9.41 Acceleration (see 3.7.40).

4.9.41.1 Acceleration (nonoperating) (when specified, see 3.1) (see 3.7.40.1). The oscillator shall be tested in accordance with MIL-STD-202, method 212. The following details shall apply:

a. Test condition C (unless otherwise specified, see 3.1).

b. Acceleration level: As specified (see 3.1).

c. Measurements: Unless otherwise specified (see 3.1).

(1) Before test: As specified in 4.9.37.

(2) After test: As specified in 4.9.2, 4.9.5, 4.9.20, and 4.9.37.

4.9.41.2 Acceleration (operating) (when specified, see 3.1) (see 3.7.40.2). The energized oscillator shall be subjected to an acceleration test as follows:

The acceleration shall be produced using a centrifuge or similar machine. A steady-state acceleration shall be applied at the specified level for the specified duration. Measurements shall be made at 5 equally spaced acceleration levels between 20 percent of the maximum and the maximum specified. The following details shall apply:

a. Acceleration level: As specified (see 3.1).

b. Acceleration duration: As specified (see 3.1).

c. Measurements: Unless otherwise specified (see 3.1).

(1) Before test: As specified in 4.9.37.

(2) During test: As specified in 4.9.5, 4.9.18.1, and 4.9.20.

(3) After test: As specified in 4.9.37.

References

1. R. L. Filler, "The Acceleration Sensitivity of Quartz Crystal Oscillators: A Review," IEEE Trans. on Ultrasonics, Ferroelectrics and Frequency Control, pp. 297-305, 1988.

2. W. P. Hanson, and T. E. Wickard, "Acceleration Sensitivity as a Function of Temperature," Proc. of the 43rd Ann. Symp. on Frequency Control, pp. 427-432, 1989, IEEE Catalog No. 89CH2690-6.

3. W. J. Riley, Jr., "The Physics of the Environmental Sensitivity of Rubidium Gas Cell Atomic Frequency Standards," IEEE Transactions on Ultrasonics, Ferroelectrics, and Frequency Control, Vol. 39, pp. 232-240, 1992.

4. T. J. Lynch, and W. J. Riley, "Tactical Rubidium Frequency Standard (TRFS)," Final Technical Report, RADC-TR-87-166, Vol. 1, 1987, AD-A192981.

5. T. M. Kwon, and T. Hahn, "Improved Vibration Performance in Passive Atomic Frequency Standards by Servo-Loop Control," Proc. of the 37th Ann. Symp. on Frequency Control, pp. 18-20, 1983, AD-A136673.

6. T. M. Kwon, B. C. Grover, and H. E. Williams, "Rubidium Frequency Standard Study," RADC-TR-83-230, Final Technical Report, Rome Air Development Center, Oct. 1983, AD-A134713.

7. T. M. Kwon, R. Dagle, W. Debley, H. Dellamano, T. Hahn, J. Horste, L. K. Lam, R. Magnuson, and T. McClellan, "A Miniature Tactical Rb Frequency Standard," Proc. of the 16th Annual Precise Time and Time Interval Applications and Planning Meeting, pp. 143-155, Nov. 1984.

8. C. Audoin, V. Candelier, and N. Dimarcq, "A Limit to the Frequency Stability of Passive Frequency Standards due to an Intermodulation Effect," IEEE Transactions on Instrumentation and Measurement, Vol. 40, pp. 121-125, April 1991.

9. C. Audoin, N. Dimarcq, and V. Giordano, "Physical Origin of the Frequency Shifts in Cesium Beam Frequency Standards Related Environmental Sensitivity," Proc. of the 22nd Annual Precise Time and Time Interval Applications and Planning Meeting, pp. 419-440, 1990, AD-A239372.

10. E. M. Mattison, "Physics of Systematic Frequency Variations in Hydrogen Masers," IEEE Transactions on Ultrasonics, Ferroelectrics, and Frequency Control, pp. 250-255, 1992.

11. "IEEE Standard Definitions of Physical Quantities for Fundamental Frequency and Time Metrology," IEEE Std 1139-1988, The Institute of Electrical and Electronics Engineers, Inc., 345 East 47th Street, New York, NY 10017, USA.

12. S. R. Stein and J. R. Vig, "Communications Frequency Standards," in: The Froehlich/Kent Encyclopedia of Telecommunications, Vol. 3 (F. E. Froehlich and A. Kent, eds.), Marcel Dekker, Inc., New York, 1992, pp. 445-500. A reprint of this chapter is available under the title "Frequency Standards for Communications," as U.S. Army Laboratory Command Technical Report SLCET-TR-91-2 (Rev. 1), October 1991, NTIS Accession No. AD-A243211.

13. P. Renoult, E. Girardet, and L. Bidart, "Mechanical and Acoustic Effects in Low Phase Noise Piezoelectric Oscillators," Proc. of the 43rd Ann. Symp. on Frequency Control, pp. 439-446, 1989, IEEE Catalog No. 89CH2690-6.

14. R. D. Weglein, "The Vibration-Induced Phase Noise of a Visco-Elastically Supported Crystal Resonator," Proc. of the 43rd Ann. Symp. on Frequency Control, pp. 433-438, 1989, IEEE Catalog No. 89CH2690-6.

15. J. R. Vig, J. W. LeBus, and R. L. Filler, "Chemically Polished Quartz," Proc. of the 31st Ann. Symp. on Frequency Control, pp. 131-143, 1977, AD-A088221.

16. R. L. Filler, L. J. Keres, T. M. Snowden, and J. R. Vig, "Ceramic Flatpack Enclosed AT and SC-cut Resonators," Proc. of the 1980 IEEE Ultrasonics Symposium, pp. 819-824, 1980.

17. R. L. Clark and M. K. Yurtseven, "Spurious Signals Induced by Vibration of Crystal Filters," Proc. IEEE Ultrasonics Symp., pp. 365-368, 1988, IEEE Catalog No. 88CH2578-3.

18. R. C. Smythe, "Acceleration Effects in Crystal Filters - a Tutorial," IEEE Transactions on Ultrasonics, Ferroelectrics, and Frequency Control, Vol. 39, pp. 335-340, May 1992.

19. "MIL-O-55310, Military Specification, Oscillators, Crystal, General Specification for," the latest revision is available from: Military Specifications and Standards, 700 Robbins Ave., Bldg. 4D, Philadelphia, PA 19111-5094.

20. R. Brendel, C. El Hasani, M. Brunet, and E. Roberts, "Influence of Magnetic Field on Quartz Crystal Oscillators," Proc. of the 43rd Ann. Symp. on Frequency Control, pp. 268-274, 1989, IEEE Cat. No. 89CH2690-6.

21. D. J. Healy, III, H. Hahn, and S. Powell, "A Measurement Technique for Determination of Frequency vs. Acceleration Characteristics of Quartz Crystal Units," Proc. of the 37th Ann. Symp. on Frequency Control, pp. 284-289, 1983, AD-A136673.

22. M. M. Driscoll, "Quartz Crystal Resonator G Sensitivity Measurement Methods and Recent Results," IEEE Transactions on Ultrasonics, Ferroelectrics, and Frequency Control, Vol. 37, No. 5. pp. 386-392, September 1990.

23. M. H. Watts, E. P. EerNisse, R. W. Ward, and R. B. Wiggins, "Technique for Measuring the Acceleration Sensitivity of SC-cut Quartz Resonators," Proc. of the 42nd Ann. Symp. on Frequency Control, pp. 442-446, 1988, AD-A217275.

24. Occupational Safety and Health Administration, 29 CFR Ch. XVII, para. 1910.95, "Occupational noise exposure," 1 July 1987.

25. W. Tustin, and R. Mercado, Random Vibration in Perspective, Tustin Technical Institute, Inc., 1984.

26. D. S. Steinberg, Vibration Analysis for Electronic Equipment, John Wiley & Sons, 1988.

27. C. M. Harris, ed., Shock and Vibration Handbook, 3rd ed., McGraw-Hill, NY, 1988.

28. T. S. Payne, "Improved Tactical Miniature Crystal Oscillator," First Interim Report, SLCET-TR-86-0011-1, U.S. Army Laboratory Command, Fort Monmouth, New Jersey, November 1987, AD-B124235. The section of this report that deals with the vibration sensitivity of crystal filters was prepared by W. Horton and P. Morley.